# 1

# Emerging "Green" Materials and Technologies for Electronics

*Melanie Baumgartner[1,2], Maria E. Coppola[3,4], Niyazi S. Sariciftci[5], Eric D. Glowacki[6], Siegfried Bauer[1], and Mihai Irimia-Vladu[3]*

[1] *Johannes Kepler University Linz, Department of Soft Matter Physics, Altenberger Str. Nr. 69, 4040, Linz, Austria*
[2] *Johannes Kepler University Linz, Institute of Polymer Science, Altenberger Str. Nr. 69, 4040, Linz, Austria*
[3] *Joanneum Research Forschungsgesellschaft mbH, Department of Materials, Franz-Pichler Str. Nr. 30, 8160, Weiz, Austria*
[4] *Politecnico di Milano, Department of Chemistry, Materials and Chemical Engineering "Giulio Natta", Piazza Leonardo da Vinci 32, 20133, Milano, Italy*
[5] *Johannes Kepler University Linz, Department of Physical Chemistry, Linz Institute for Organic Solar Cells, Altenberger Str. Nr. 69, 4040 Linz, Austria*
[6] *Linköping University, Norrköping campus, Laboratory of Organic Electronics, Department of Science and Technology, Bredgatan 33, Norrköping 60174, Sweden*



## 1.1 Introduction to "Green" Materials for Electronics

We are currently witnessing an evolution of technologies blurring the lines between the physical, digital, and biological spheres. Electronics become highly flexible and even mechanically stretchable, with applications ranging from wearable consumer electronics to mobile health, sports, and well-being. The materials aspects of flexible and stretchable electronics is covered in depth by many pioneers in the field, summarizing also the latest developments spanning from stretchable interconnects to the level of highly sophisticated electronic skin [1–5]. A wide class of materials is available in thin film forms, ranging from dielectrics and semiconductors to metals, as well as a cornucopia of industrially relevant processing methods. Initial attempts toward biocompatible electronics paved the way toward epidermal [6] and implantable electronics [7–9]. Sustainable use of material resources is a major concern of our society, challenging research with the ever-growing amount of electronic waste, estimated to be 41.8 million metric tons (Mt) at the end of 2014 and forecasted to reach 50 million Mt by 2018 [10].

Inspiration from nature led to the first approaches to biodegradable forms of electronics, finally culminating in the development of transient electronics that simply degrades after service life [11]. The state of the art in "green" electronics has been summarized in a recent review, covering degradable substrates and materials for encapsulation, as well as dielectrics, semiconductors, and metals for basic electronic circuit elements [12]. In this chapter we will provide a brief overview on "green" materials for degradable circuit boards and organic electronics, including the latest developments in the field. We first summarize

*Green Materials for Electronics*, First Edition.
Edited by Mihai Irimia-Vladu, Eric D. Glowacki, Niyazi S. Sariciftci, and Siegfried Bauer.

the use of paper, followed by a discussion of natural and nature inspired materials, including DNA and nucleobases; silk; saccharides; Aloe Vera, natural waxes, and gums; cellulose and its derivatives; resins; proteins, peptides, and amino acids; and finally natural and nature-inspired semiconductors for biodegradable and biocompatible electronics. We expect that in the future we will be as comfortable with highly flexible and degradable forms of electronics, embedded everywhere, in textiles, on skin, and even within our body as we are now familiar with smartphones and tablet computers.

## 1.2 Paper

More than 2000 years ago the Chinese inventive genius brought to light what is to date of incommensurable importance for humanity: paper, a natural-origin and sustainable (renewable and degradable) material. Good tunable physical properties, such as transparency or roughness, make paper desirable for large-area products. Paper wins over other flexible substrate materials owing to its low cost (below 0.1 USD $m^{-2}$), high flexibility, and the possibility for large-scale roll-to-roll manufacturing with speeds of processing exceeding 25 m $s^{-1}$ [13]. When the cultivation of wood, the basic material for paper, is executed environmentally sustainably and when recycled paper is used in the fabrication process, paper outrivals most candidates for substrates in biodegradable devices. Apart from its classic usages for packaging, information storage, and as support for displays, paper recently developed into a substrate for a wide variety of unconventional electronics. Paper electronics is continuously drawing attention in the scientific community and is highlighted in this book extensively in Chapter 6 by Martti Toivakka *et al.* for a plethora of applications. In the following, we will only briefly present the usage of paper as substrate and dielectric for basic electronic circuits. Martins *et al.* have utilized, for example, both the above-mentioned assets of paper in a low power electronic Complementary Metal-Oxide-Semiconductor (CMOS) inverter circuit layered on a flexible and recyclable fiber-based paper substrate. The paper gate dielectric offers a large capacitance per area at low frequencies because of its fiber-based foam-like structure. Figure 1.1a displays an image of a CMOS inverter on paper, tested under different supply voltages. Figure 1.1b shows the voltage transfer characteristics (*VTC*s) of the inverters, which are used to extract the high and low states, associated with the input and output voltages. Gain and leakage current are extracted from Figure 1.1c [14]. Although the reported results are not impressive in terms of CMOS performance, the use of paper for a dual function of substrate and dielectric is highly promising since it enables layering of various semiconductor structures (dielectrics and semiconductors). The demonstration opens the door for implementing paper for a plethora of applications that can be broadly grouped under the umbrella of "green" electronics (memory elements and integrated systems, smart labels, tags, sensors, and electrochromic paper displays, to name a few).

The rough surface of paper, combined with its high absorbance tendency for various liquids, makes very challenging the processing of solution-based active layers on top of it. Pettersson *et al.* eliminated the problem of semiconductor absorption into the paper substrate by using a mixture containing a semiconductor

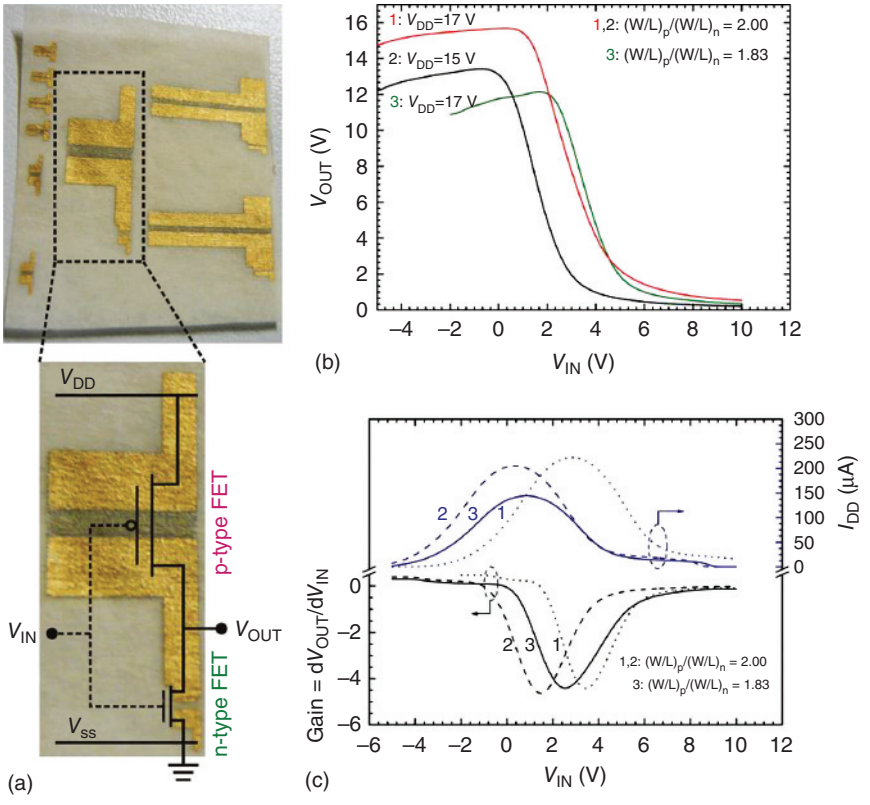


**Figure 1.1** The potential of paper for the fabrication of future CMOS architectures: (a) photograph of a low-power electronic CMOS inverter circuit on paper; (b) the voltage transfer characteristics of the CMOS inverters; and (c) the gain, $dV_{out}/dV_{in}$, and the leakage current, $I_{DD}$. (Martins *et al*. 2011 [14]. Reproduced with permission of John Wiley and Sons.)

and a biodegradable polymer insulator [15]. In this compound, spontaneous phase separation occurs, and a thin semiconducting layer is formed on top (Figure 1.2Aa). Owing to this preparation step, the sensitive semiconductor was separated from the paper substrate. Importantly, the rough surface of paper does not play an important role anymore, in that it does not transpose its unevenness through the dielectric and to the dielectric–semiconductor interface where the charge transport occurs. Another aspect of utmost importance is the stability of devices fabricated on paper. Pettersson *et al*. examined the bias–stress stability and the shelf life of transistors on paper [16]. These transistors were connected in advanced circuits, including NOR gates and D-latches. Stabilities of up to 3 weeks were observed, currently limiting the usage of such paper electronic devices to short-term applications only. To prove the operation principle, a logic NOR-gate was fabricated with two transistors and one 5.6 MΩ resistor. For NOR gates, a high output (i.e., value of 1) results if both the inputs to the gate are low (i.e., both display a value of 0). Figure 1.2B shows the output of such logic circuit device with a low operating voltage and fast switching of the states, from one state to the other [16].

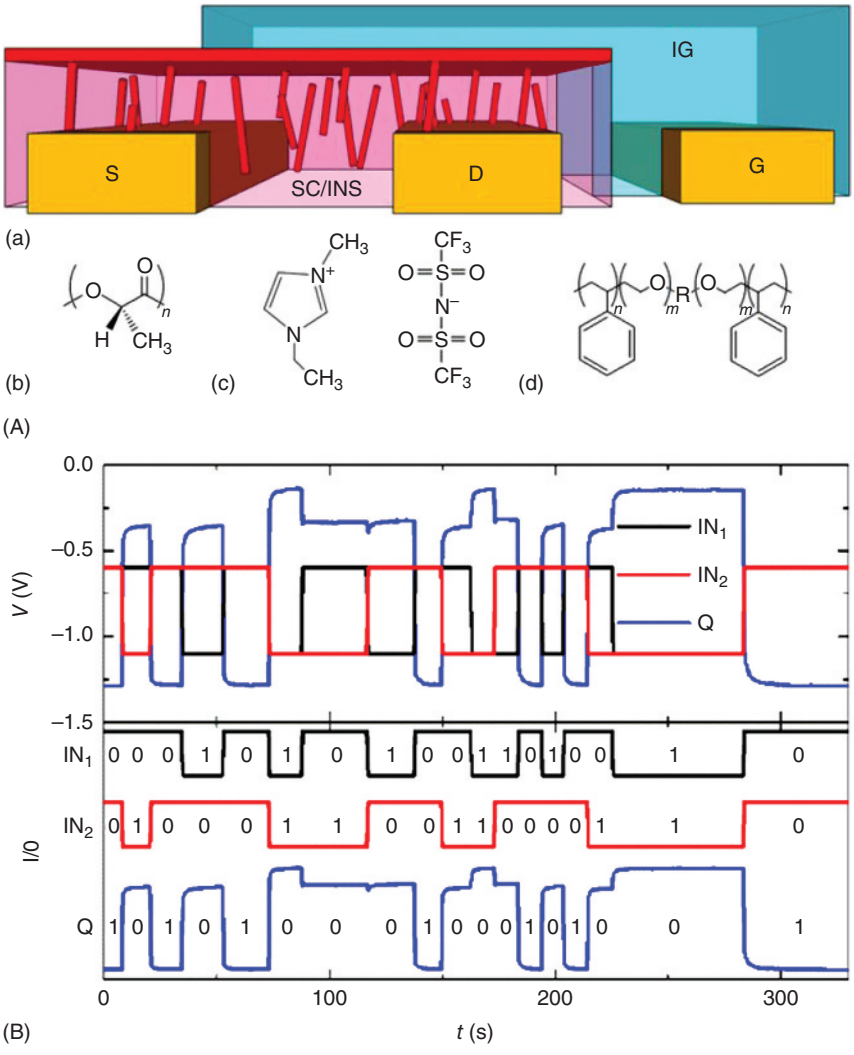


**Figure 1.2** (A) (a) Schematic of the OFET structure containing the gate (G), source (S), and drain (D) electrodes, the ion gel (*IG*,) and the self-separating semiconductor insulator blend (SC/INS); (b) the chemical structure of the poly(L-lactic acid) (*PLLA*); (c) the chemical structure of the ion gel used, 1-ethyl-3-methylimidazolium bis(trifluoromethylsulfonyl)imide (EMIM:TFSI); and (d) the chemical structure of the triblock copolymer, PS:PEO:PS (7 wt%), used as a gelling agent for the ion gel. (Pettersson *et al*. 2014 [15]. Reproduced with permission of Cambridge University Press.). (B) Output data of the NOR-gate with a supply voltage, $V_{DD}$, of −1.3 V. The raw signals are superimposed in the top graph and presented deconvoluted in the bottom graph. (Pettersson *et al*. 2015 [16]. Reproduced with permission of John Wiley and Sons.)

Paper, although a challenging material for device preparation, opens the door to low-cost disposable electronics. Electronic devices fabricated on paper will need also a power supply, and for such purpose paper-based photovoltaics could be a perfect complement. Paper appears to be an ideal support material for photovoltaic cells,

being ~1000 times less expensive than glass and ~100 times less expensive than common plastics. Barr *et al.* demonstrated the potential of unmodified paper for photovoltaics fabrication [17]. The paper photovoltaic arrays reported by the group generated impressive performance: an open circuit voltage approaching 50 V and a current of ~10 μA capable of powering electronic displays under ambient indoor lighting for at least 6000 h of uninterrupted power supply. Moreover, the photovoltaic arrays could be tortuously flexed and folded without loss of function. In 2014 Leonat *et al.* showed that nearly doubling the Power Conversion Efficiency (PCE) (i.e., reaching efficiencies of 4%) compared to the one reported in reference [17] for an individual polymer-based photovoltaic cell on paper is possible [18]. Figure 1.3a displays the component materials used in the fabrication process of the organic solar cell on a double-side coated image printer paper that is displayed in Figure 1.3b.

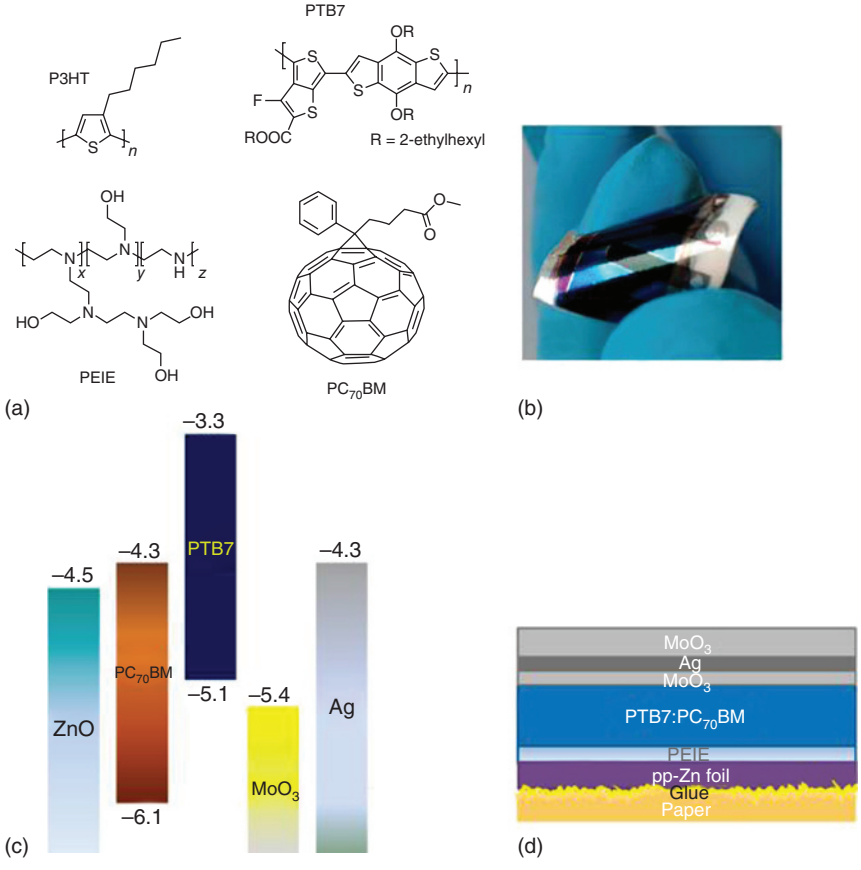


**Figure 1.3** (a) Chemicals employed in bulk fabrication of heterojunction solar cell devices: standard P3HT and novel PTB7 polymers as electron donors; $PC_{70}BM$ as electron acceptor; polyethylenimine (*PEIE*) deposited in a thin layer (10 nm) coating to improve the work function and injection of ZnO back electrode; (b) photograph of a 4% efficient organic solar cell on a flexible paper support; (c) energetic levels of the photovoltaic layers; (d) schematic of the fabricated device showing the sequence of the layers. (Leonat *et al.* 2014 [18]. Reproduced with permission of American Chemical Society.)

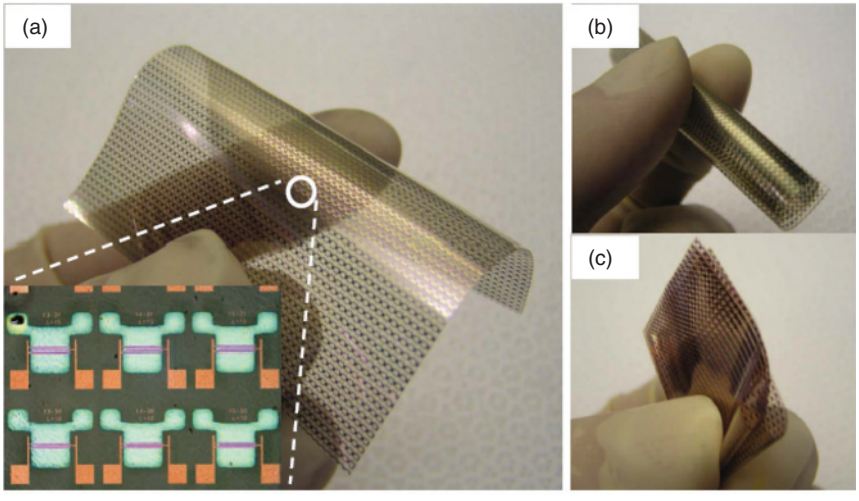


(A)

| | 1 | 2 | 3 | 4 | 5 | 6 | 7 | 8 | 9 | 10 | Mobility | No. of TFTs |
|---|---|---|---|---|---|---|---|---|---|---|---|---|
| A | 0.24 | 0.19 | 0.30 | 0.25 | 0.21 | 0.26 | 0.22 | 0.24 | 0.04 | 0.13 | 0.00 – 0.04 | 7 |
| B | 0.23 | 0.00 | 0.29 | 0.21 | 0.28 | 0.35 | 0.40 | 0.14 | 0.19 | 0.20 | 0.05 – 0.09 | 5 |
| C | 0.34 | 0.36 | 0.26 | 0.24 | 0.36 | 0.48 | 0.26 | 0.44 | 0.21 | 0.26 | 0.10 – 0.14 | 7 |
| D | 0.16 | 0.29 | 0.22 | 0.16 | 0.01 | 0.00 | 0.40 | 0.35 | 0.06 | 0.39 | 0.15 – 0.19 | 12 |
| E | 0.14 | 0.35 | 0.45 | 0.43 | 0.43 | 0.28 | 0.02 | 0.34 | 0.19 | 0.23 | 0.20 – 0.24 | 19 |
| F | 0.16 | 0.20 | 0.22 | 0.38 | 0.36 | 0.30 | 0.02 | 0.34 | 0.05 | 0.19 | 0.25 – 0.29 | 16 |
| G | 0.16 | 0.36 | 0.11 | 0.27 | 0.40 | 0.33 | 0.57 | 0.23 | 0.13 | 0.38 | 0.30 – 0.34 | 10 |
| H | 0.16 | 0.47 | 0.12 | 0.24 | 0.18 | 0.24 | 0.38 | 0.04 | 0.29 | 0.23 | 0.35 – 0.39 | 12 |
| I | 0.27 | 0.34 | 0.24 | 0.06 | 0.14 | 0.27 | 0.17 | 0.05 | 0.56 | 0.17 | 0.40 – 0.44 | 7 |
| J | 0.34 | 0.33 | 0.26 | 0.44 | 0.23 | 0.32 | 0.37 | 0.07 | 0.28 | 0.25 | 0.45 – 0.49 | 3 |
| | | | | | | | | | | | 0.50 – 0.54 | 0 |
| | | | | | | | | | | | 0.55 – 0.59 | 2 |
| | | | | | | | | | | | | Σ 100 |

(B)

**Figure 1.4** (A) (a) Photograph and a magnified image by optical microscopy of transparent, nanopaper-based OTFT array. Photographs revealing the (b) bending and (c) folding deformation modes endured by the substrate. (Fujisaki *et al*. 2014 [19]. Reproduced with permission of John Wiley and Sons.) (B) Field-effect mobility map of the transistor array on 5€ paper banknote with an area of $10 \times 8\,mm^2$ showing the distribution of the field-effect mobility. (Zschieschang *et al*. 2011 [20]. Reproduced with permission of John Wiley and Sons.)

The coating is based on a zinc metalized polypropylene thin film, where propylene serves as smoothener of the rough paper surface and prevents capillary penetration of the solution-processed active layers into the paper substrate, while zinc is employed as the metallic electrode of the device. Energy band diagrams of the components and the layered sketch of the device are presented in Figure 1.3c,d respectively [18].

A next step will be the realization of truly 3D-shaped paper electronics; in this respect Kirigami techniques seem promising to make paper not only flexible but even stretchable. Highly flexible, sustainable optoelectronics may soon become a reality with the aid of highly transparent paper. Cellulose nanopaper (made from nano-sized cellulose fibers) was selected as substrate for flexible electronics, as reported by Fujisaki *et al*. [19] Initial work employed a 20 µm thin transparent paper, made from native wood cellulose nanofibers only, as substrate for fabrication of high-mobility organic thin film transistor (TFT) arrays. Figure 1.4Aa depicts a photograph and an optical microscopic image of a 20 µm thin transparent nanopaper-based OTFT array. Figure 1.4Ab,c demonstrate the amenability of the substrate material to withstand torturous deformation, in a similar way to conventional paper.

OTFT arrays might also be a good option for anti-counterfeiting and tracking feature applications, especially when printed directly on banknotes. Zschieschang *et al*. demonstrated the fabrication of complex circuits with high yield and reproducibility directly on the rough surface of paper bills [20]. Such circuits could form advanced electronic safety features for counterfeit protection (Figure 1.4B). In a recent report Kim and coworkers demonstrated for the first time one-dimensional photonic nanocavities on paper after their transfer printing with the aid of a micro-sized stamp [21].The nanocavity exhibits lasing (Figure 1.5) and displays a wavelength shift dependent on the amount of hydration of the paper substrate, proving also its amenability to function as a sensor. Although the *Q*-factor is

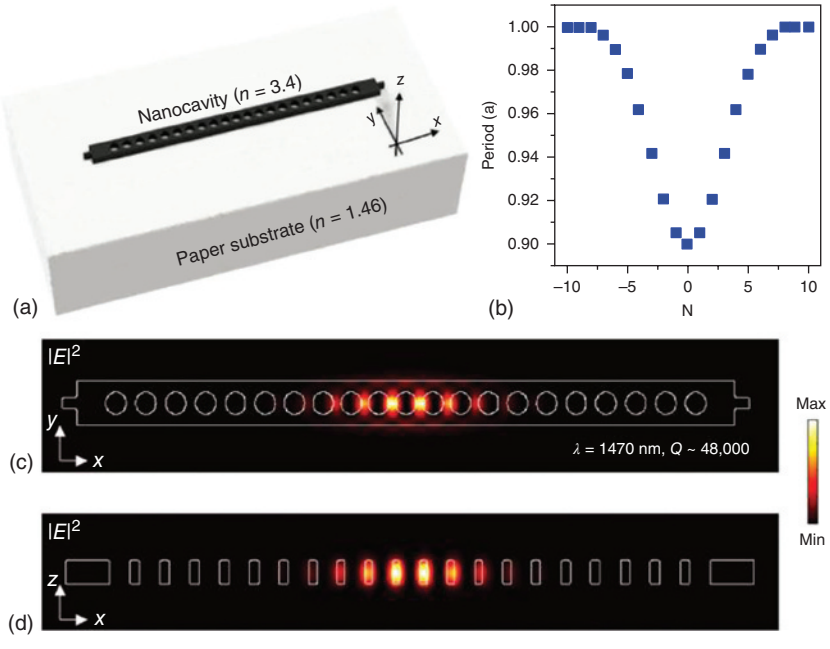


**Figure 1.5** (a) Schematic of a semiconductor photonic nanocavity laser deposited via transfer printing on a paper substrate; (b) the Gaussian-modulated period of hole-to-hole distances along the *x*-axis from 0.9a to 1.0a. (c) The electric field intensity of the photonic crystal on the *x*–*y* plane and (d) the electric field intensity of the photonic crystal on the *x*–*z* plane. (Kim *et al*. 2016 [21]. Reproduced with permission of John Wiley and Sons.)

reduced by a factor of 10 when the paper substrate is introduced as support for the free-standing nanocavity crystal, the lasing threshold remains low, at ~0.2 mW. When employing the communication wavelength of 1.55 μm, the paper substrate provides a sufficiently high *Q*-factor for lasing, potentially paving a way for telecommunication applications. The selected research examples discussed here serve to illustrate the huge potential of paper for future development of sustainable electronics and photonic devices.

## 1.3 DNA and Nucleobases

In 1953, Watson and Crick published the helical structure of deoxyribonucleic acid, better known as *DNA* [22]. This investigation led to a better understanding of the main building block of every living organism on Earth and its genetic code transmittance responsible for growth, development, functioning, and reproduction. The long fibrous DNA molecule consists of a very long backbone chain formed by repeated units of a sugar group (deoxyribose) and a phosphate group alternately bonded to nucleobase molecules (the purines adenine and guanine, and the pyrimidines cytosine and thymine). Although the DNA-based research represented from its inception the bread and butter of genomics [23], the molecule stirred increasing interest over the past decade as a material for organic electronics, in the intention to bridge functional electronics with living organisms. Yumusak *et al.* demonstrated a bio-organic field-effect transistor (*BioOFET*) based on a cross-linked DNA gate dielectric, purified from salmon waste [24]. DNA is soluble only in aqueous solutions, which makes implementation of standard processing techniques from organic solvents difficult. The authors engineered a DNA–lipid complex that became water insoluble and processible in high quality films from organic solvents using standard device fabrication techniques such as spin coating. Steckl *et al.* paved the way for using DNA in organic light-emitting diodes (*OLED*s) and emphasized the potential of DNA as an inexpensive and biodegradable source material for the development of optical waveguides and laser structures [25, 26]. Thin films of DNA incorporated into the fluorescent emitting materials for OLEDs can increase the brightness of the respective devices by one order of magnitude compared to OLEDs produced from standard materials. The authors found that the DNA layer behaves as a highly efficient electron-blocking layer (*EBL*) while not hampering hole transport. Therefore, the thin DNA layer enhances the probability of exciton formation and eventually of photon emission in fluorescent OLEDs decorated with specific fluorophores (i.e., standard AlQ3 for green and NPB for blue emission respectively) as visualized in Figure 1.6a [27]. When DNA-surfactant thin films are incorporated in phosphorescent OLEDs, the brightness and efficiency of the DNA-based devices outperforms their phosphorescent counterparts, as revealed in Figure 1.6b.

DNA capping layers also enhance charge injection in OFETs, as demonstrated by Zhang *et al.* [28]. In their work, DNA works as an interlayer for n-type and ambipolar semiconductor OFETs fabrication with gold as top source and drain electrodes. The DNA layer in the device, schematically shown in Figure 1.7Aa, allows for the injection of both charge carriers. The OFET was prepared either

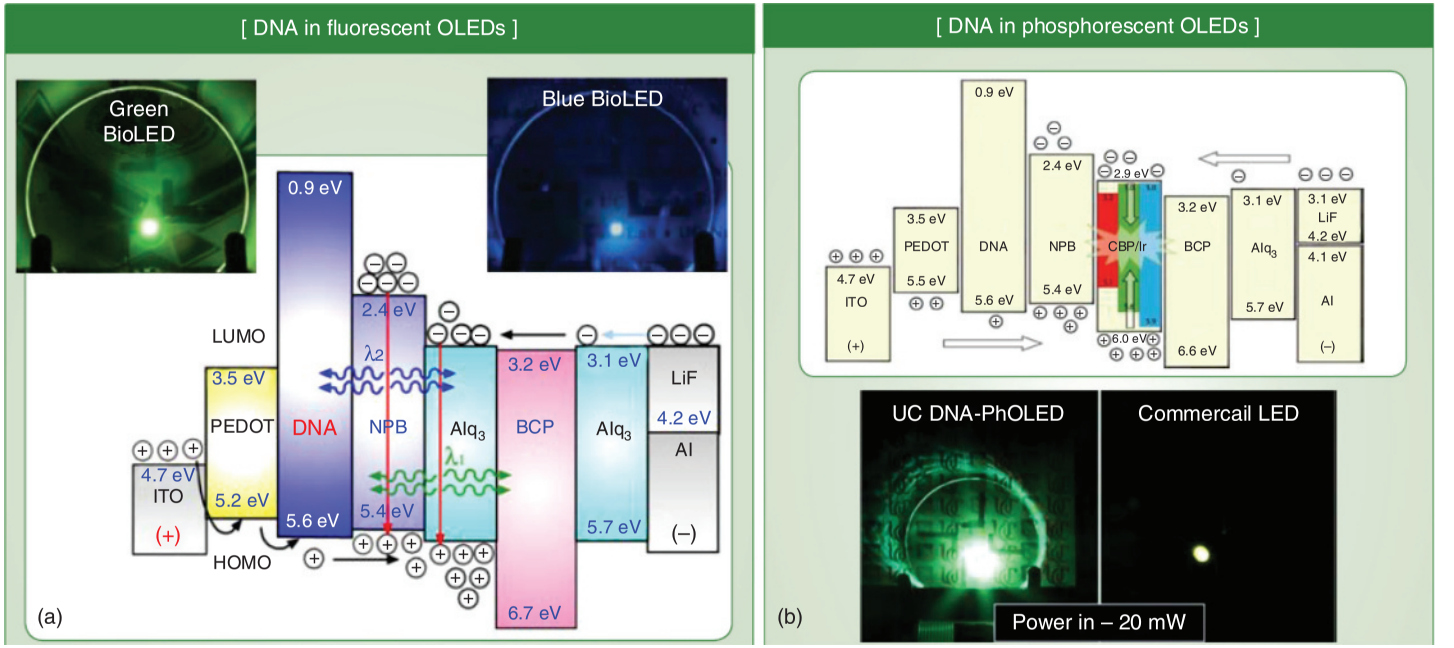


**Figure 1.6** (a) Fluorescent OLEDs with DNA surfactant as electron-blocking layer employing AlQ3 fluorophore for green emission and NPB for blue emission. The bottom schematic displays the energy diagram of the layered structure; (b) DNA surfactant employed in the fabrication of phosphorescent OLEDs: the energy diagrams (top) of the layered structure, and the comparison of DNA-based OLED with a commercially available phosphorescent LED, with both devices biased at 20 mW (bottom). (Steckl *et al.* 2011 [27]. Reproduced with permission of Optics & Photonics News.)

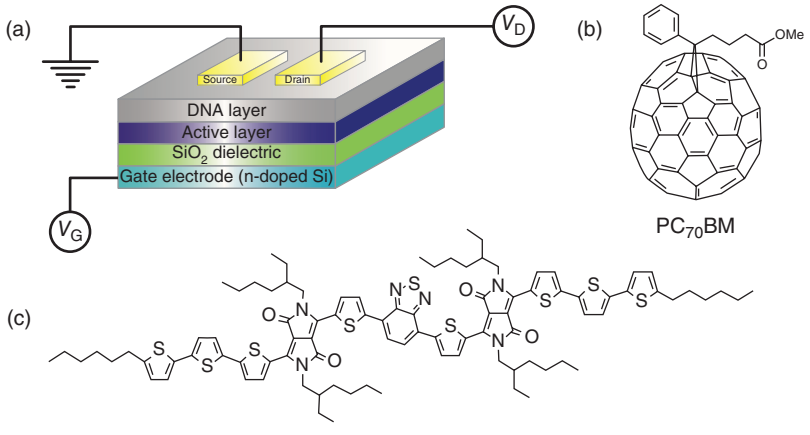


(A)

| | $\mu_{lin}$ (*e*) ($cm^2\ V^{-1}\ s^{-1}$) | $\mu_{sat}$ (*e*) ($cm^2\ V^{-1}\ s^{-1}$) | $\mu_{sat}$ (*h*) ($cm^2\ V^{-1}\ s^{-1}$) | $V_{th}$ (V)[a] |
|---|---|---|---|---|
| $PC_{70}BM$ | $7.5 \times 10^{-3}$ | $9 \times 10^{-3}$ | N/A | 16 |
| $PC_{70}BM$/DNA | $1.7 \times 10^{-2}$ | $1.6 \times 10^{-2}$ | N/A | 10 |
| BTDPP2 | $4.8 \times 10^{-4}$ | $4.4 \times 10^{-3}$ | $6 \times 10^{-3}$ | 12 |
| BTDPP2/DNA | $2.3 \times 10^{-3}$ | $1.1 \times 10^{-2}$ | $2.1 \times 10^{-2}$ | 6.5 |

(B) [a] $V_{th}$ is determined from the linear regime under electron accumulation mode.

**Figure 1.7** (A) (a) Schematic of the device structure with DNA used a charge injection layer and (b–c) chemical structure of the semiconductors employed. (Zhang *et al*. 2012 [28]. Reproduced with permission of John Wiley and Sons.) (B) Device parameters of OFETs fabricated using $PC_{70}BM$, $PC_{70}BM$/DNA, BTDPP2, and BTDPP2/DNA.

with an n-type semiconductor material, [6,6]-phenyl-$C_{71}$-butyric acid methyl ester($PC_{70}BM$) (with the structure depicted in Figure 1.7Ab) and 4,7-bis{2-[2,5-bis(2-ethylhexyl)-3-(5-hexyl-2,2′:5′,2″-terthiophene-5″-yl)-pyrrolo[3,4-*c*]pyrrolo-1,4-dione-6-yl]-thiophene-5-yl}-2,1,3-benzothiadiazole (BTDPP2) (shown in Figure 1.7Ac) or with an ambipolar semiconductor, diketopyrrolopyrrole (*DPP*). The fabricated OFETs having DNA as injection layer showed an increase in field-effect mobility of up to one order of magnitude as compared to the samples that have no such interlayer (see Figure 1.7B).

Far easier to process than DNA are its constituent nucleobases that are widely available in crystalline powder form; they can be used without purification, or alternatively can be scrupulously purified to a desired extent via the train sublimation method. AFM surface investigations of vacuum-sublimed thin films deposited on glass substrates demonstrated a root mean square (*rms*) roughness of ~3 nm for guanine, ~14.5 nm for adenine, ~24 nm for cytosine, and ~65 nm for thymine [29]. The authors showed that ultrathin layers of natural adenine, guanine, thymine, and cytosine can be used as stand-alone dielectric or in combination with one another in alternating layers.

Irimia-Vladu *et al.* widely investigated the use of various such permutations that were reported in several publications [29–31]. For example, four alternating layers of adenine and guanine as dielectric in a fully biodegradable and biocompatible OFET were implemented, resulting in a specific capacitance of 5.1 nF $cm^{-2}$, stemming from a calculated dielectric constant of ~3.85 for adenine and ~4.35 for guanine measured at 1 kHz. The authors showed that in spite of the final roughness of the combined layer, the alternating adenine and guanine films produce an insulator that is sufficiently dense to work as dielectric layer in OFETs fabricated on a variety of biodegradable substrate materials: hard gelatine, caramelized sugar, or even on ecological nursery foils [30]. Because nucleobases are amenable for thin-film processing by vacuum deposition, they are ideally suited as thin capping layers for dipole-rich metal oxide dielectric interfaces. Figure 1.8

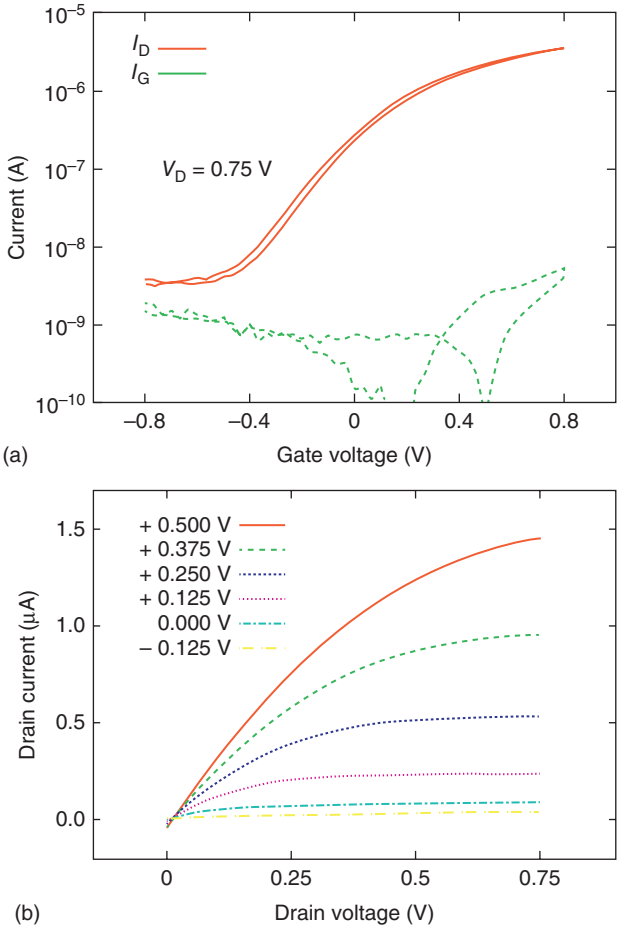


**Figure 1.8** (a) Transfer and (b) output characteristics of a low-operating voltage OFET with adenine employed as capping layer on electrochemically grown aluminum oxide layer. Hot wall epitaxial-deposited $C_{60}$ acts as organic semiconductor and aluminum as contact electrodes. (Schwabegger *et al.* 2011 [32]. Reproduced with permission of Elsevier.)

shows such an example through the transfer and output characteristics of an $AlO_x$–adenine gate dielectric. A thin film of vacuum processed adenine was used by the authors as a capping layer for the electrochemically grown aluminum oxide layer, resulting in a combined organic–inorganic dielectric having a high specific capacitance of ~0.1 μF cm$^{-2}$ and consequently contributing to a remarkable field-effect mobility of the hot-wall epitaxially deposited fullerene $C_{60}$ organic semiconductor of ~3.4 cm$^2$ V$^{-1}$ s$^{-1}$ [32].

Nucleobases showed promising applications not only in OFETs but also in organic light-emitting diodes, OLEDs. Gomez *et al*. investigated the nucleobases thymine (T) and adenine (A) as EBLs that lead to a high photoemission efficiency in OLEDs [33]. In their following work they also included guanine (G), cytosine (C), and uracil (U) into the investigation as EBL as also as hole-blocking layer (*HBL*) in the OLED structure along with a thorough study of their thin-film and electronic properties [34]. Nucleobases have similar Highest Occupied Molecular Orbital (HOMO)–Lowest Unoccupied Molecular Orbital (LUMO) energy gaps as DNA (i.e., ranging from 3.6 to 4.1 eV), but differently, they have a fairly large range of electron affinity values (1.8–3.0 eV) that allow for an additional degree of freedom in device design. Table 1.1 summarizes the peak performance of different nucleobases tested as EBL and HBL.

**Table 1.1** Performance summary of the investigated nucleobases as electron-blocking layers (EBL) and hole-blocking layers (HBL) in organic light-emitting diodes.

| | Turn-on (V) | Maximum luminance (cd m$^{-2}$) | Maximum current efficacy (cd A$^{-1}$) | Maximum luminous efficacy (lum W$^{-1}$) | Quantum efficiency (%) | |
|---|---|---|---|---|---|---|
| | | | | | Ext | Int |
| *(a) EBL type II* | | | | | | |
| Baseline | 3.25 | 95.179 | 38.5 | 22.3 | 10.7 | 59.4 |
| **G** | 4.75 | 17.191 | 44.3 | 21.9 | 12.3 | 68.3 |
| **A** | 5.0 | 82.289 | 51.8 | 21.2 | 14.3 | 79.4 |
| **C** | 5.0 | 5.646 | 36.1 | 14.5 | 10.0 | 55.6 |
| **T** | 7.75 | 3.844 | 22.6 | 6.9 | 6.3 | 35.0 |
| **U** | 7.0 | 21 | 3.3 | 1.2 | 0.9 | 5.0 |
| DNA–CTMA | 3.75 | 60.061 | 43.3 | 25.6 | 12.0 | 66.7 |
| *(b) HBL type III* | | | | | | |
| **G** | 6.0 | 16 | 1.3 | 0.6 | 0.4 | 2.2 |
| **A** | 5.5 | 215 | 1.0 | 0.4 | 0.3 | 1.6 |
| **C** | 5.5 | 217 | 5.2 | 2.1 | 1.5 | 8.3 |
| **T** | 5.5 | 362 | 15.1 | 5.0 | 4.2 | 23.3 |
| **U** | 4.25 | 4 045 | 16.3 | 7.4 | 4.6 | 25.6 |

*Source*: Gomez *et al*. 2015 [34]. Reproduced with permission of John Wiley and Sons.

For the devices tested as HBL/ETL, uracil performed the best of all nucleobases as HBL, having the largest current, the best efficiency, and the highest luminance. C-based OLEDs display both EBL and HBL tendencies. For the devices tested as HBL/EBL, uracil performed the best of all nucleobases as HBL, having the largest current, the best efficiency, and the highest luminance.

With the above exemplified reports, the door now stands widely open for the employment of DNA and its constituent nucleobases in the field of electronics. Low cost and easy process routines make DNA and its nucleobases interesting and appealing for interfacing electronics with living matter. Particularly its use in sensing and optoelectronics is very promising, and perhaps soon DNA will add one more word to its denomination of "molecule of life"; it could become "the molecule of light" [27].

## 1.4 Silk

When the production of silk in woven fibers was implemented in China more than 3500 years BC, the shiny precious material was reserved only for local aristocracy. Later on it found its way through the silk road to Europe's royalty and wealthy class. Silk is naturally produced from hundreds of different silkworm species, with the mulberry silkworm as its most famous representative [35]. Today silk is not only desired for fashion purpose, rather more as an interesting part of research, especially in the fields of tissue engineering and regenerative medicine because of its biocompatibility stemming mainly from its protein constituency [36]. Owing to its biodegradability and biocompatibility, silk has also come into the focus of organic electronics in recent years for a wide range of applications. Hota *et al*. used natural silk fibroin protein to fabricate a transparent biomemristor and investigated the endurance and retention characteristics of the device [37]. As proved in Figure 1.9a, metal–insulator–metal (*MIM*) capacitors with silk fibroin protein showed memory resistor and rectifying characteristics at the same time, and were therefore memristive in nature. The schematic design of the device is shown in the insets of the figure. In Figure 1.9b the retention characteristics of the memristor device is shown, with attainable switching ratios of approximately 10–11 times.

The dynamic mechanical and dielectric properties of amorphous regenerated films of silk fibroin were studied by Magoshi and Magoshi in 1975 [38]. In 2011 Wang *et al*. fabricated a flexible organic thin-film transistor with a silk fibroin gate dielectric by coating a thin layer of silk fibroin film onto a Polyethylene terephthalate (PET) substrate patterned with a gold gate electrode [39]. The silk dielectric had to be dip-cast to achieve a continuous layer. Pentacene was thermally evaporated onto the dry silk film for the organic semiconductor layer and the device was finalized with gold as source and drain contacts. Figure 1.10a shows a photograph of the rollable pentacene OTFT and in Figure 1.10b the transfer characteristics of the device are presented, displaying a very small hysteresis, indicative of a very low level of charge trap density at or near the pentacene–silk fibroin interface [39]. Another example for silk as dielectric in organic electronics was offered by the work of Capelli *et al*. who integrated silk protein in OFETs and organic light-emitting transistors (*OLET*s) respectively, with the latter devices yielding a light

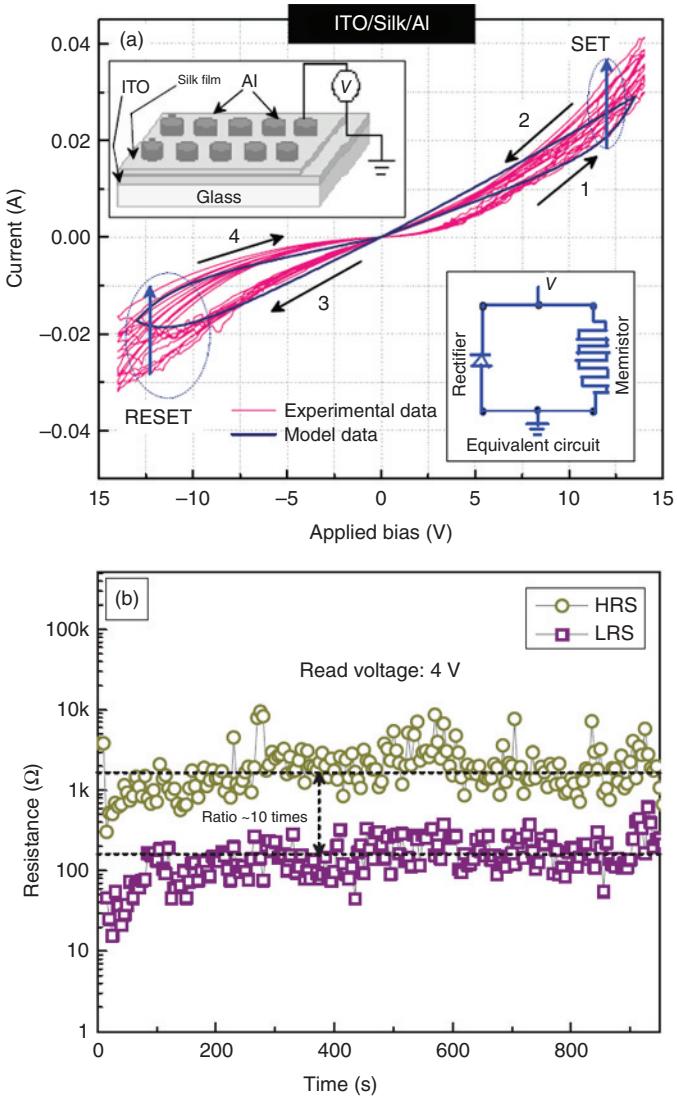


**Figure 1.9** (a) Reversible and nonvolatile switching characteristics of memristor devices with silk fibroin protein showing good match between the experimental and the model data and (b) retention test of the high resistance states (*HRS*) and low resistance states (*LRS*) of the ITO/silk/Al capacitor structures under a positive bias operation, with resistances read at 4 V. (Hota *et al*. 2012 [37]. Reproduced with permission of John Wiley and Sons.)

emission of 100 nW [40]. In a more recent publication, Chang *et al*. employed major ampulate spider silk as polyelectrolyte gate dielectric for OFETs with pentacene semiconductor and analyzed the important role of hydration of the silk dielectric for obtaining reproducible results at different levels of relative humidity [41]. Various other research groups harvested the excellent properties of silk, such as flexibility, good mechanical properties, and the ability to stand alone as a film, and employed it in the development of organic electronic devices. One such

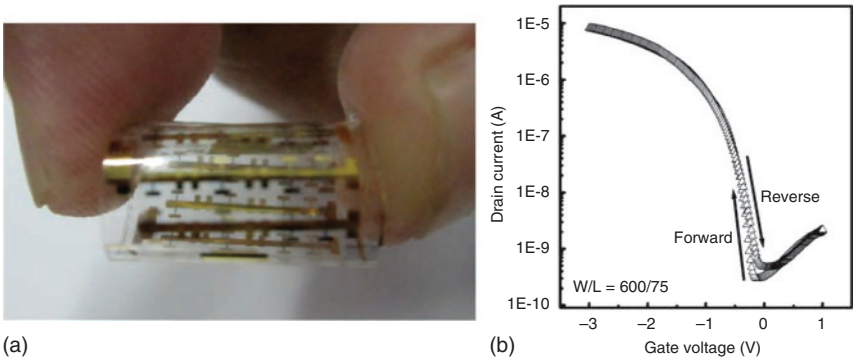


**Figure 1.10** (a) Photograph of the rollable OTFT with pentacene semiconductor and silk fibroin gate dielectric and (b) transfer characteristics of the transistor. (Wang *et al*. 2011 [39]. Reproduced with permission of John Wiley and Sons.)

example was offered by Kim *et al*. who presented in their work an interesting way to transfer metal electrodes to a thin, freestanding silk film [42].

Figure 1.11 shows the process routine of the transfer printing with a schematic diagram on the left and a corresponding high-resolution image on the right and optical microscopy images of the circuits in the insets. In the fabrication sequence described in Figure 1.11, metal oxide field-effect transistors were first placed on a Poly(methyl methacrylate (PMMA) carrier wafer. Afterwards the devices where lifted on a poly(dimethylsiloxane) *PDMS* stamp, displayed in Figure 1.11b. With this setup the electrodes could be transferred to a silk film on a silicon wafer (Figure 1.11c) or even to a freestanding silk film (Figure 1.11d), thereby contributing to the development of bioresorbable electronics. In a follow-up report of the same group, Hwang *et al*. designed devices capable of interfacing electronics with living tissue for biomedical applications [43]. In their work, silk with various degrees of crystallinity was used as a programmable dissolving substrate and encapsulation for a wide series of devices. The group demonstrated transistors, diodes, inductors, capacitors, and resistors, all made out of thin active layers of magnesium and magnesium oxides, silicon nanomembranes and silicon dioxides, with controllable transient times dictated by the controlled dissolution of silk encapsulate and substrates. In several follow-up contributions, the group of John Rogers cemented the indispensability of silk in the development of transient electronics. The respective field is covered extensively by Huang and Rogers in Chapter 5 of this book.

Another interesting approach was to employ silk fibers and dye them with a conducting conjugated polyelectrolyte, as shown by Müller *et al*. [44]. The group fabricated an electrochemical transistors (*ECT*s) by arranging the coated fibers in a simple cross-junction configuration. Conducting fibers could be woven into pristine fiber segments. Intelligent clothing with silk fibers will surely be an exciting option for the future. The good insulating properties and its simple processibility from aqueous solutions make silk a good alternative as dielectric for electronic devices. The highest potential of silk lies in its good programmability of its dissolution in liquids, notably in bodily fluids, and these amazing characteristics have secured the use of silk in the fabrication recipes of future transient electronic devices.

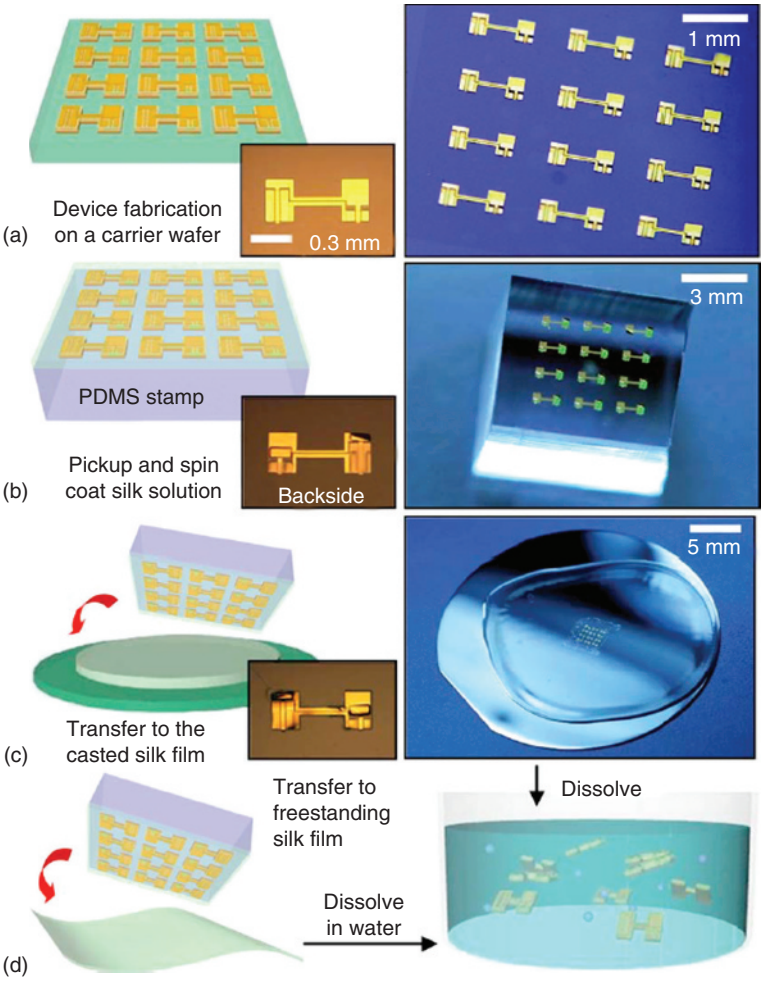


**Figure 1.11** (a) (left) Schematic diagram and the microscope image as inset of devices fabricated on carrier wafer; (right) high-resolution image of the ultrathin devices on a carrier wafer; (b) devices lifted onto the surface of a PDMS stamp; (c) spin coating of thin silk film on silicon wafer onto which the devices are transferred; and (d) (left) transfer printing onto a freestanding silk film and (right) dissolution of the devices. (Kim *et al*. 2009 [42]. Reproduced with permission of AIP Publishing.)

## 1.5 Saccharides

Sweet things come to our mind, when we hear the word sugar. Sugar molecules have a long history in chemistry and biochemistry and were first reported more than 250 years ago [45]. This substance of plant origin can be grouped into three categories: monosaccharides, such as fructose, glucose, and galactose; disaccharides, such as lactose, maltose, and sucrose; and finally oligosaccharides. When targeting the fabrication of biodegradable and biocompatible electronics, the simplest small molecules of the sugar family are highly eligible, owing to their nontoxicity, good

acceptance in society, and simple processing routes from aqueous solvents. Irimia-Vladu *et al*. investigated the dielectric properties of spin-coated glucose and lactose films and their applicability in OFETs. Solution-processed sugars have excellent film-forming properties. Such spin cast films show an rms roughness in the range of 0.5–1 nm, which helps in the subsequent deposition of high-quality layers of semiconductors and contact electrodes [29, 30]. The measured specific capacitance of a 2.6 μm thick film cast from a glucose solution in deionized water was 2.15 nF $cm^{-2}$. The film of glucose was employed as dielectric layer in the fabrication of OFETs; Figure 1.12 shows transfer and output characteristics of such an OFET with fullerene $C_{60}$ acting as the semiconducting layer [29]. In another

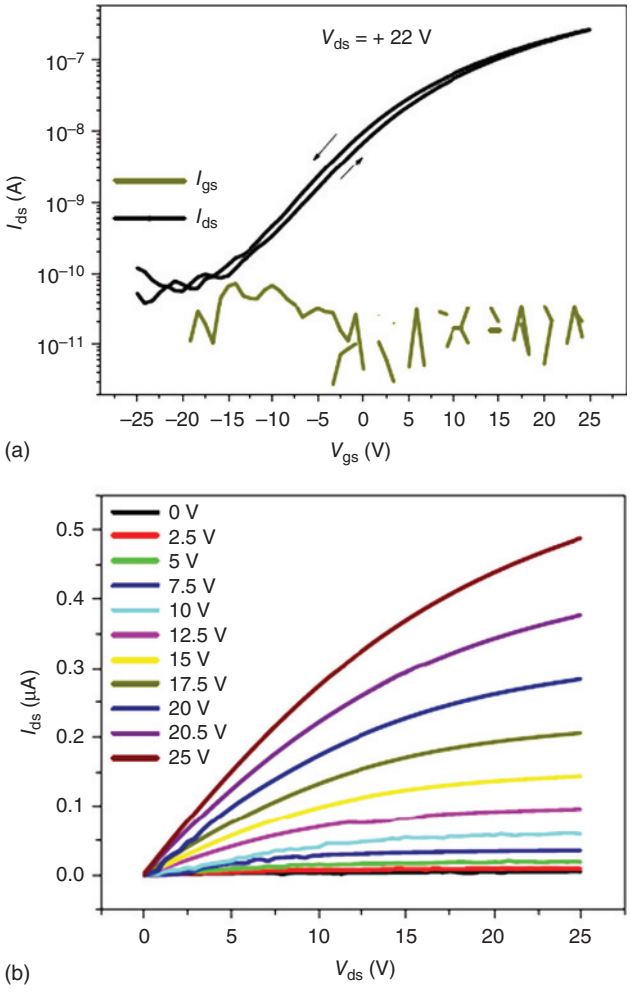


**Figure 1.12** Transfer (a) and output (b) characteristics of an OFET with solution-processed glucose gate dielectric and $C_{60}$ semiconductor channel showing minimal hysteresis and excellent insulating characteristics (very low leakage currents) of glucose dielectric. (Irimia-Vladu *et al*. 2010 [29]. Reproduced with permission of Elsevier.)

**Table 1.2** Mechanical properties of the investigated polymer composite samples of gelatine (G) and sucrose (S) in Poly(vinyl alcohol) (PVA) matrix.

| Sample | Ultimate Stress (MPa) | Tensile Strain at Break (%) | Young's Modulus (MPa) |
|---|---|---|---|
| PVA | 40.5 ± 2.9 | 76 ± 9.2 | 1304.8 ± 218.5 |
| 0.1 G | 115.6 ± 17.1 | 2.6 ± 0.6 | 3022.7 ± 378.7 |
| 0.5 G | 42.4 ± 2.7 | 4.3 ± 0.7 | 1699.9 ± 167.9 |
| 1 G | 41.2 ± 5.3 | 1.9 ± 0.2 | 1384.5 ± 107.8 |
| 2 G | 50.7 ± 12.1 | 3.7 ± 0.9 | 1182.7 ± 64.7 |
| 0.1 S | 40.6 ± 3.6 | 184.4 ± 19.6 | 513.9 ± 40.8 |
| 0.5 S | 22.1 ± 1.1 | 313.7 ± 8.3 | 45.7 ± 2.3 |
| 1 S | 21.7 ± 1.9 | 419.1 ± 22.1 | 28.7 ± 4.2 |
| 2 S | 7.1 ± 1.4 | 333.1 ± 34.5 | 8.7 ± 0.8 |

*Source*: Acar *et al*. 2014 [46]. Reproduced with permission of John Wiley and Sons.

contribution, the same group showed that caramelized glucose is also an appropriate substrate for organic electronic devices [30].

Other research groups have tried to take advantage of the plasticizing effect of sugars in combination with polymers. Acar *et al*. integrated sucrose in a polymer matrix to fabricate a tunable material for transient electronics [46]. The addition of sucrose shifted the glass transition temperature ($T_g$) to lower temperatures, which resulted in more elastic composites at temperatures above $T_g$. Table 1.2 lists the Young's modulus, tensile strength, and tensile strain at break measured from the stress–strain curves. Increasing the concentration of sucrose in the Poly(vinyl alcohol) (PVA)/sucrose composite also increases the solubility of the resulting compound, which recommends the blend as an ideal candidate for the development of programmable transient materials for biomedical applications.

Sugar can play a major role in organic electronics, especially in transient electronics, because of its nontoxicity, good water solubility, low cost, and easy processibility. The sugar family has many members, besides the already mentioned ones, that still wait for close investigation and implementation in organic electronics, such as ribose, the inner constituent of DNA molecules.

## 1.6 Aloe Vera, Natural Waxes, and Gums

*Aloe barbadensis miller*, better known as *Aloe Vera*, is a succulent plant growing in the dry regions of Africa, Asia, and Americas. A variety of ancient cultures used the plant for medical treatment and as a skin care product. In traditional medicine, Aloe Vera gel is widely used as anti-inflammatory drug for the relief of sunburns or insect bites. The fleshy Aloe Vera leaves contain an inner clear gel that consists up to 99% of water. The remaining 1% includes glucomannans,

amino acids, lipids, sterols, and vitamins [47]. Aloe Vera as an active layer in electronic devices is cost efficient, easy to process, and suitable for biodegradable and biocompatible devices. Aloe Vera found its way into electronics development through the work of Khor and Cheong who investigated the dielectric properties of commercially purchased Aloe Vera gel. The group found a dielectric constant of ~3.4 for a screen-printed Aloe Vera layer [48]. Based on this knowledge they built an n-type OFET. In Figure 1.13a, the schematic design of the OFET is presented, including the dielectric layer consisting of a mixture of extracted natural Aloe Vera paste from fresh leaves with added 1.5 wt% of $SiO_2$ nanoparticles. The $SiO_2$ nanoparticles were introduced in order to enhance the compatibility of the semiconductor, $C_{60}$ with the Aloe Vera gel. Figure 1.13b shows the output characteristic of the device with the first measurement taken immediately after its fabrication and the second one after 14 days. Stored under ambient condition, the OFET showed diminished device performance explained by the authors as a change in hydration of the dielectric layer; but it could be also largely credited to the oxidation of the semiconductor layer and of the contact electrodes [49].

Other materials of plant origin that found applicability in organic electronics development are natural gums and waxes. Gum Arabic, also known as *acacia gum*, segregates from various species of acacia trees. Ancient Egyptians already knew of the good adhesive properties of gum Arabic and used it in combination with mineral pigments for paintings [50, 51]. Nowadays, gum Arabic is widely employed in food industry as an ingredient of chewing gum. Gum mastic, another natural gum used for more than 2500 years in traditional Greek medicine, is obtained from the mastic tree, *Pistacia lentiscus* [52]. Nowadays, this brittle and translucent resin is still used in folk medicine and food industry. Another plant-derived exudate is carnauba wax, mostly harvested in Brazil from the palm tree *Copernicia cerifera*. It is the hardest natural wax that melts at ~80–87 °C and is usually added to other waxes to increase their melting point. It is also used for encapsulation in pharmacy and food industry owing to its excellent water repellent properties [53]. In the field of organic electronics these materials are very suitable as dielectrics when either hydrophilic (gums) or hydrophobic (waxes) layers are sought for device development. Stadlober *et al*. studied a variety of natural-origin materials for bioelectronics, such as gum Arabic, gum mastic, paraffin, beewax, and carnauba wax [54]. The dielectric constant measured at 1 kHz is 2.9 for carnauba wax and higher for the materials processed from aqueous solutions, that is, 4.1 for gum Arabic and 3.9 for gum mastic. In combination with a hybrid gate dielectric, such as electrochemically grown aluminum oxide ($Al_2O_3$), the gums and the waxes form a sufficiently dense and highly insulating gate dielectric. They also show excellent surface characteristics to assist the growth of the subsequently deposited organic semiconductor layer of OFETs. Figure 1.14Aa shows the output and transfer characteristics of a pentacene OFET with a hybrid bilayer dielectric of gum Arabic on $Al_2O_3$, assisting in obtaining a high mobility of 0.56 $cm^2 V^{-1} s^{-1}$ for the pentacene semiconductor [54]. In another report, Glowacki *et al*. combined the naturally occurring oligo ethylene, tetratetracontane (*TTC*), with aluminum oxide for obtaining a hybrid organic–inorganic dielectric layer and

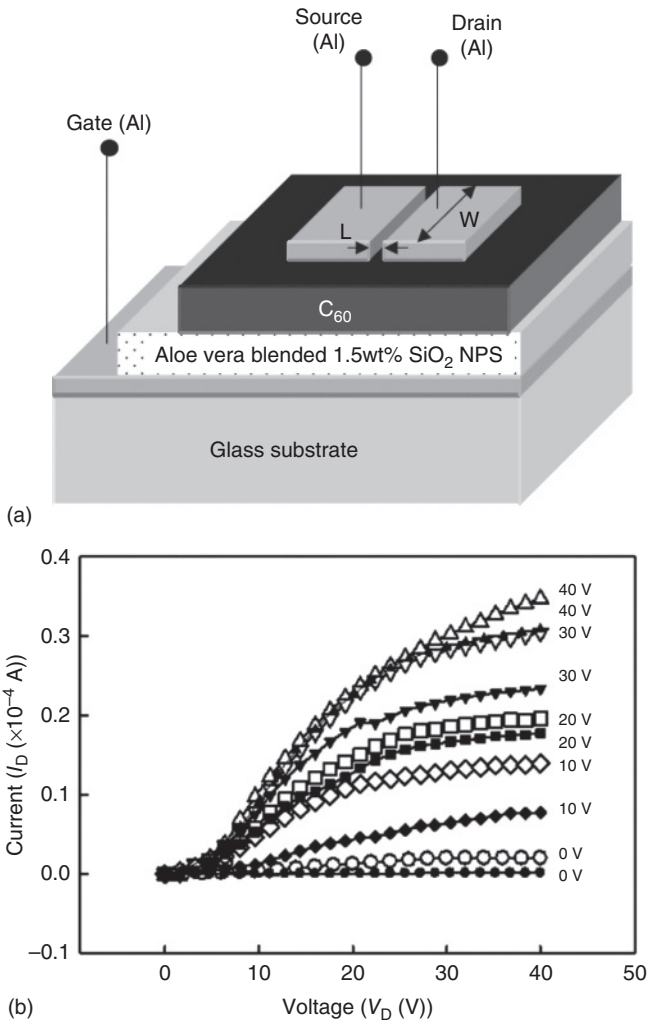


**Figure 1.13** (a) Schematic of the employed architecture for the fabrication of OFETs with Aloe Vera gate dielectric including 1.5 wt% $SiO_2$ filler and (b) output characteristics of one representative device showing the initial measurement (open symbols) and the one recorded after 14 days (filled symbols). The significant drop in output current is presumably due to changes in the hydration level of the dielectric layer, with oxidation of the semiconductor and contact electrodes that could have also played a role. (Qian Khor and Cheong 2013 [49]. Reproduced with permission of The Electrochemical Society.)

the hydrogen-bonded semiconducting pigment quinacridone in OFET devices [55]. This air-stable semiconductor pigment quinacridone shows a very high $T_{80}$ value of its mobility retention (time elapsed so that the mobility decreases to 80% of its initial value), as shown in Figure 1.14B, and can be operated in air without significant degradation for at least 140 days [55].

The main advantage of all these above exemplified materials, as well as of many other waxes and gums that wait to be reported for the organic electronics

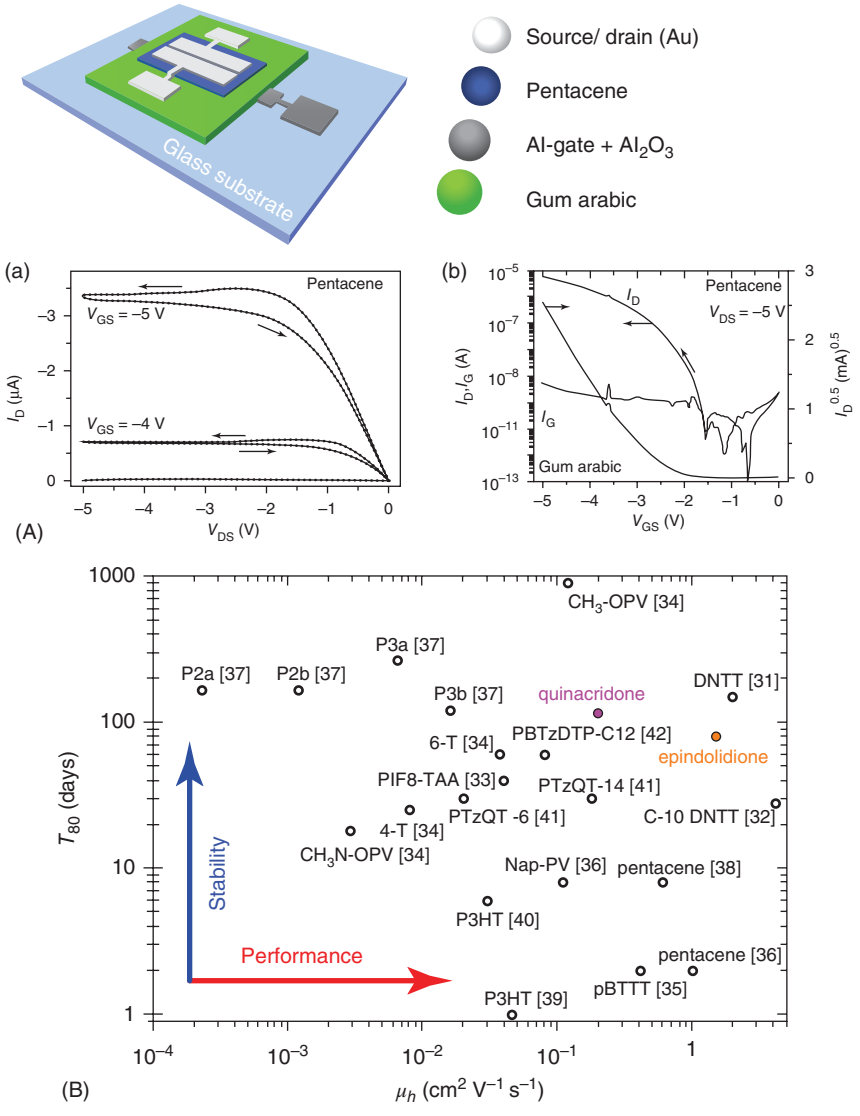


**Figure 1.14** (A, top) Schematic of the fabricated OFET with gum Arabic capping layer on $Al_2O_3$ dielectric and pentacene semiconductor; (A, a,b) transfer and output characteristics of the device, which shows minimal hysteresis and high mobility of the organic semiconductor. Stadlober *et al*. 2015 [54]. Reproduced with permission of IEEE.; (B) degradation time $T_{80}$, expressed in days required for the mobility of the organic semiconductor to drop to 80% of its initial value. Devices with polyethylene oligomer, tetratetracontane (i.e., $C_{44}H_{90}$) dielectric showed impressive performance with epindolidione and quinacridone semiconductors. (Glowacki *et al*. 2013 [55]. Reproduced with permission of John Wiley and Sons.)

development, is their low cost and easy processibility. All gums are processible from aqueous solvents, whereas waxes are amenable for doctor blading or screen-printed deposition technique in their melted form.

## 1.7 Cellulose and Cellulose Derivatives

Cellulose as a carbohydrate surpasses the non-carbohydrate lignin for the position of the most prominent biopolymer on Earth, and is one of the most substantial biomass materials. Cellulose-first an integral part of papyrus and later of paper-was indirectly employed by the humanity to document events and spread its knowledge; cellulose became part of ascending research interest over the past 150 years. Some highlights regarding the implementation of cellulose in electronics will be offered below. Good dielectric properties make cellulose ideal as dielectric in complex circuit designs and also as substrate for circuits in general [56]. In fact, one of the most noticeable properties of cellulose to be harvested in bioelectronics is its high dielectric constant for an organic material [57]. Unfortunately, its high molecular weight and complexity make cellulose difficult to process in significant amounts in virtually any type of solvent. Attaching functional groups to impart solubility to cellulose was demonstrated by Petritz *et al.* who investigated the solution processible cellulose derivative tri-methyl silyl cellulose *TMSC* as an ultrathin dielectric film for complementary inverter fabrication [58]. The group employed a hybrid organic–inorganic dielectric containing electrochemically grown aluminum oxide, $Al_2O_3$, and TMSC as capping layer for the inverter fabrication, and showed that TMSC alone can function with good performance too. Figure 1.15a shows the performance of such a complementary inverter circuit as VTCs and gain curves for an operation window between 0 and 7 V. Figure 1.15b displays the noise margin (*NM*) and mismatch $\Delta V_M$ of the threshold voltage $V_M$ as a function of the supply voltage, whereas Figure 1.15c exemplifies the "maximum equal criterion" method to extract the noise margin by displaying the maximum size of a square that fits between the inverter curve and the mirrored inverter curve [58]. Owing to its excellent smoothness and low trap density characteristics, the TMSC dielectric contributed to recording of impressive gains in excess of 1000 and noise margins over 90% for a low operating voltage of the complementary inverter circuit. The significant degree of hydrophobicity of cellulose derivative TMSC was harvested by the same group in a follow-up publication demonstrating the functionality of a complementary-like inverter based on a single type of ambipolar semiconductor (6,6′-Cl-Indigo) [59]. Another approach is the utilization of cellulose in cellulose-based ionogels as high capacitance gate dielectric for the fabrication of electrolyte-gated field-effect transistors on paper, as shown in the report of Thiemann *et al.* [60]. In this case, the gate dielectric of the TFT is a thin flexible electrolyte film that is ionically conducting but highly electronically insulating, rendering its superior dielectric properties to cellulose ionogel that has a high specific capacitance varying from 4.6 to 15.6 $\mu F\,cm^{-2}$. Figure 1.16a shows a schematic illustration of electrolyte-gated TFT with ZnO nanorods semiconductor and a lateral gate on multilayer-coated paper with laminated cellulose ionogel as dielectric; Figure 1.16b displays the optical image of a ZnO nanorod TFT on multilayer-coated paper. The fabricated TFTs turn on at 0.8 V and have on/off ratios of about 100, as presented in Figure 1.16c. Owing to the flexibility of the paper, the TFT samples could also be measured during inward bending as shown in Figure 1.16d, with a slight degradation recorded during a compressive strain test.

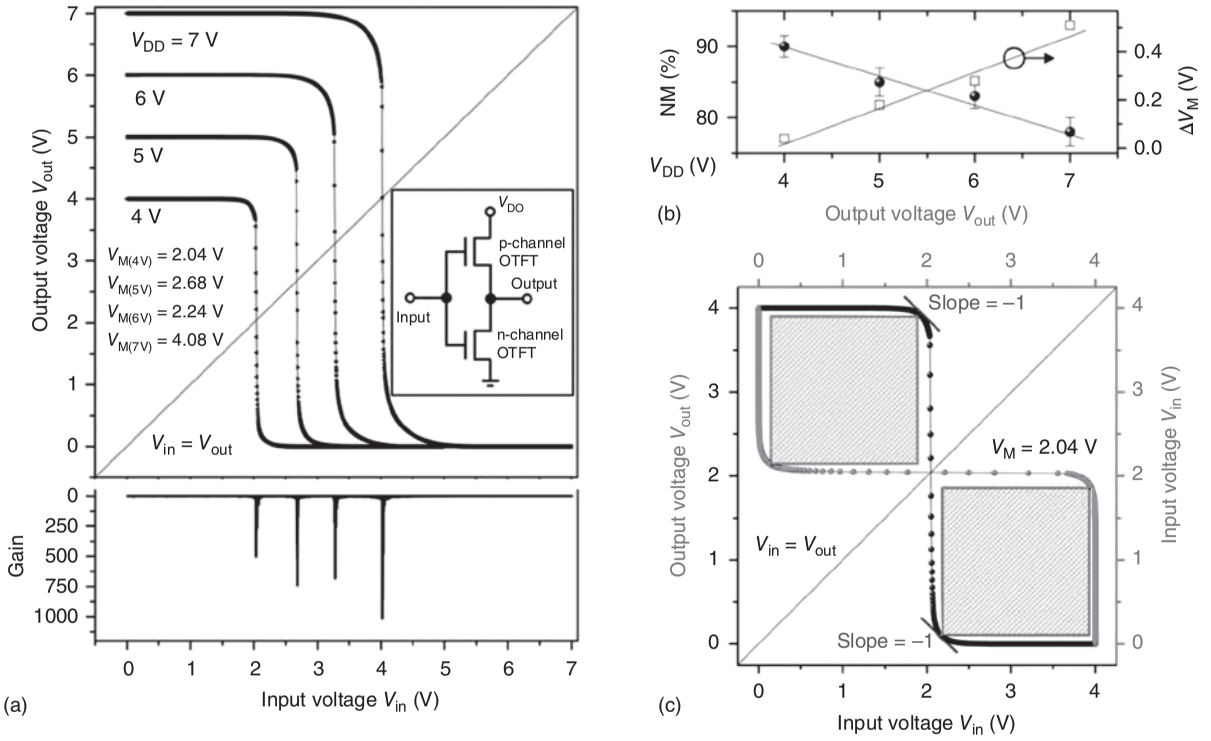


**Figure 1.15** (a) Inverter performance expressed as voltage transfer curves (*VTC*s) for a complementary inverter with fullerene, $C_{60}$, and pentacene as organic semiconductors and TMSC-$Al_2O_3$ dielectric. The bottom graph displays the measured gain that reached 1600 for a champion device; (b) the noise margin (NM) and the mismatch $\Delta V_M$ of the threshold voltage as a function of the supply voltage; and (c) "maximum equal criterion," the method employed for noise margin estimation by calculating the maximum size of a square that fits between the inverter curve and the mirrored inverter curve, at a supply voltage $V_{DD}$ of only 4 V [58]. (Petritz *et al*. 2015, http://onlinelibrary.wiley.com/doi/10.1002/adma.201404627/full. Used under CC-BY-4.0 http://creativecommons.org/licenses/by/4.0/.)

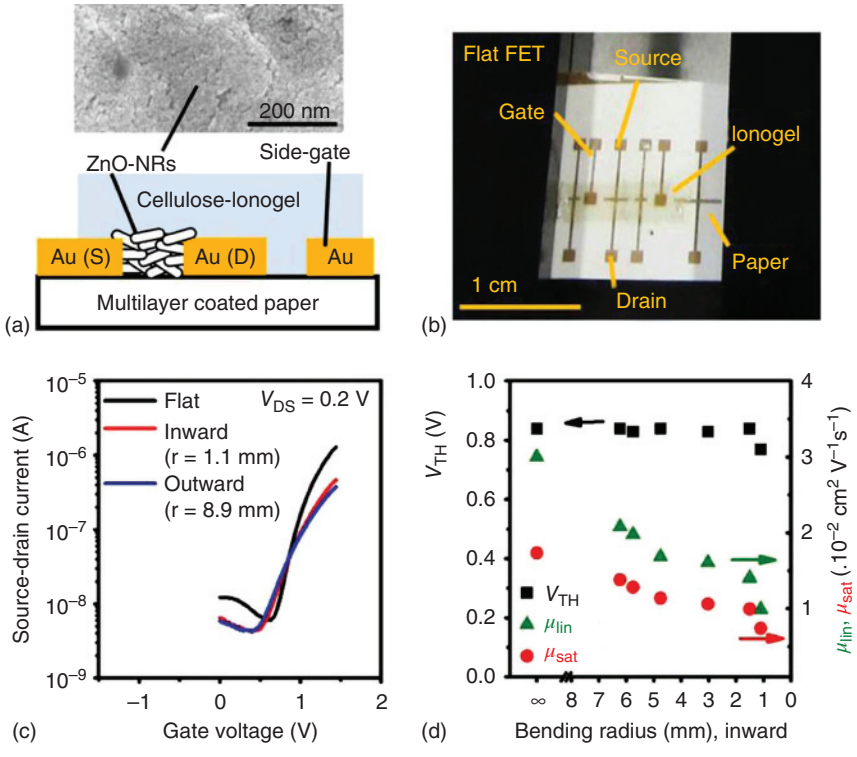


**Figure 1.16** (a) Schematic of electrolyte-gated TFT structure with ZnO nanorods and side gate fabricated on multilayer-coated paper with laminated cellulose ionogel; the inset displays a scanning electron microscopy image of the short ZnO nanorods (typical length ~14 nm) on paper; (b) image of the tested device taken before the bending test; (c) transfer characteristics of the TFT recorded before and during inward and outward bending tests (radius 1.1 and 8.9 mm respectively) at a drain–source voltage $V_{ds}$ = 0.2 V; and (d) threshold voltages ($V_{th}$) and field-effect mobilities (calculated in the linear and the saturated regimes) versus the inward bending radius. (Thiemann *et al.* 2013 [60]. Reproduced with permission of John Wiley and Sons.)

Beside its good dielectric properties, cellulose is highly suitable as substrate for organic electronics. Transparency, lightweight, and flexibility are the key properties of cellulose that Gomez and Steckl harvested for the fabrication of OLEDs [61]. The goal of that research was to pave the way for the fabrication of OLEDs based on fully natural materials. Figure 1.17 shows the schematic device that has adenine as the hole injection layer on a cellulose/epoxy substrate.

With respect to the substrates, especially nanocellulose-based paper sheets show very good transparency and smoother surfaces than regular paper. This material is highly biocompatible and therefore suitable for medical applications, which in combination with electronics could lead to improved diagnostic monitoring for patients [62]. The combination of the technical use of nanocellulose and electronics is considerable. Cellulose nanopapers are well suited as ultrafiltration membranes [63]. Evaporated electronics could, for example, monitor the durability of the filter and give notice when the filter has to be changed.

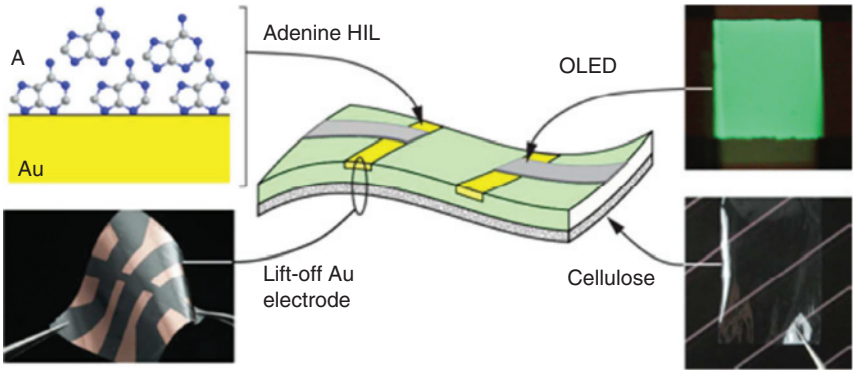


**Figure 1.17** Device structure of an OLED with cellulose substrate, gold electrode, and adenine as hole injection layer. (Gomez and Steckl 2015 [61]. Reproduced with permission of American Chemical Society.)

One interesting avenue to follow will be the investigation of bacterial cellulose, which is different than plant cellulose in that it is more chemically pure, has ultrafine network architecture, contains no hemicellulose or lignin, and has a higher hydrophilicity and better tensile strength. Bacterial grown cellulose can be molded in any form and shape owing to the degrees of freedom offered by the polymerization reaction [64]. The dawn of implementation of cellulose in organic electronics has arrived and it will be interesting to see how this "green" and abundant material will find applications targeting sustainable developments for electronics.

## 1.8 Resins

A resin is a natural material either of plant or animal origin. Plant resins are generally referred to as *sap* or *sticky exudates* and are lipid-soluble mixtures of volatile and nonvolatile terpenoid and/or phenolic secondary compounds that are usually secreted in specialized structures located either internally or on the surface of the plant and have potential significance in ecological interactions. Irrespective of their origin (plant or animal), natural resins are traditionally classified into three main classes: hard resins (as copal, shellac or mastic), soft resins (as frankincense and myrrh), and oleoresins (mainly from Pinaceae genus), including turpentines, balsams, and elemis. Most of the resins belonging to these three classes have attracted deep interest for their medicinal properties and/or have been exploited in the industrial production of varnishes and lacquers and in the preparation of incenses and perfumes. Often mistaken with other plant exudates, that is, gums, the resins are fundamentally different. While gums are complex polysaccharides mixtures that decompose completely upon heating without melting, resins melt and progressively release volatile oils when the temperature is increased over their melting point [65]. As a rule of thumb, resins are processible in alcoholic solutions but insoluble in water, whereas gums are exactly the opposite; another class of exudates is formed by gum resins, which are to some extent a mixture of the two

and are soluble to some degree in both types of solvents exemplified above [66]. Typical building blocks of most of the resins produced by plants are terpenes and terpenoids, organic compounds widespread in nature as constituents of essential oils as well as major components of turpentine, the fluid obtained by the distillation of resins mainly from trees belonging to the pine family. Most prominent examples of plant resins are amber and copal, which are listed in most of the physics textbooks as examples of highly insulating materials. Although natural resins secreted by plants are overwhelming in their numbers, animal origin resins also exist. An example of animal origin resin with industrial significance is shellac, which is secreted by one tiny insect, *Tachardia Lacca* (with its subspecies *Kerria Lacca* and *Kerria Chinensis*) and deposited on the branches of insect colonies supporting trees in India, Thailand, and China. This red insect produces an excretion that acts as protective coating for its larvae against UV radiation. The amber-colored substance known as *lac* is the raw material of shellac manufacture that sums up to 20 000 tons per year worldwide [67, 68]. Most popular for its use as binder for phonograph records of the 78 rpm era, it is nowadays employed mostly as barrier coating to prevent moisture loss in citric fruits (its major worldwide application) as well as enteric coating for medical capsules intended to pass unaffected the upper part of the gastrointestinal tract and probe the colon [69]. In 1979 Goswami investigated the dielectric behavior of the constituents of the natural resin shellac [70] and in the year 2013, Irimia-Vladu *et al*. employed shellac as dielectric in OFETs [71]. Fresh shellac flakes readily dissolve in alcoholic solvents, preferably ethanol, and can be processed into films of different thickness via either drop casting or spin coating. Those drop cast or spin-coated layers can be cross-linked by heating the samples, not exceeding a temperature of 100 °C, with a resulting film displaying remarkable surface smoothness [71, 72]. In one such investigation, Irimia-Vladu *et al*. prepared a 30 nm shellac dielectric layer in an OFET device and also a 500 μm thick shellac substrate. Impressive smoothness of the film with rms roughness of ~1 nm revealed by AFM investigations, coupled with the absence of dipolar or ionic relaxation mechanisms in the frequency range of $10^{-3}$–$10^{4}$ Hz demonstrated by means of dielectric spectroscopy, make shellac ideal for utilization in organic electronics [71]. Figure 1.18a,b shows the transfer characteristics of (a) a $C_{60}$ OFET and (b) a pentacene OFET fabricated on a 500 μm thick drop cast shellac substrate, with 250 nm thin shellac as gate dielectric layer. In both cases, the devices showed no hysteresis, indicating that the trap density for electrons or holes at the semiconductor interface is negligibly small. Shellac is versatile and easily modifiable chemically, so future applications in organic electronics are likely to come. In addition, a wide range of resins of plant origin still await investigation and implementation in electronic devices. In a pioneering work, Coppola *et al*. investigated a large number of plant-origin resins as dielectrics for OFET fabrication: amber, copal, frankincense, mhyrr, damar, sandarac, guggul, spruce, cedar, rosin, mastic, and elemi (Coppola *et al*., manuscript in preparation). Two examples of such investigation are presented in Figure 1.18c,d for spruce and myrrh dielectrics in OFETs with pentacene semiconductor. An interesting feature of all the resins investigated is the absence or occurrence of very minimal hysteresis in OFETs, an astonishing feat that happens in spite of their chemical complexity and composition diversity.

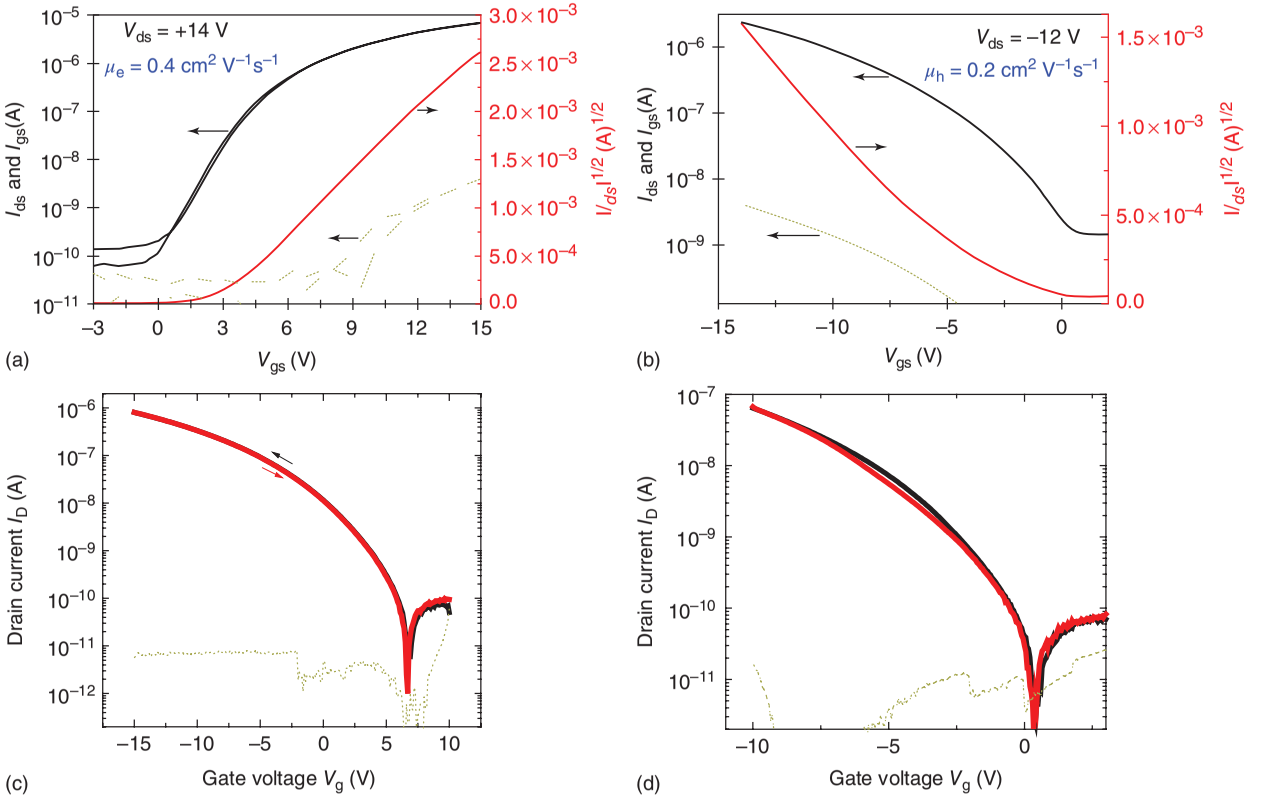


**Figure 1.18** Hysteresis-free OFETs with natural resins processed from ethanol (~200–250 nm thick films) and used as capping layer of 32 nm thick aluminum oxide dielectric. (a) OFET with Shellac as capping layer on aluminum oxide dielectric and fullerene semiconductor; (b) OFET with Shellac as capping layer on aluminum oxide dielectric and pentacene semiconductor (Irimia-Vladu *et al.* 2013 [71]. Reproduced with permission of The Royal Society of Chemistry.); (c) spruce resin, and (d) myrrh resin as dielectrics processed from ethanol with vacuum-deposited pentacene as organic semiconductor in both cases.

## 1.9 Gelatine

Gelatine is a widely used common commodity material with a very long history. Studies show that ancient Egyptians already boiled bone and animal leather, which contained natural collagen as glue. Scientists assume however that the knowledge of the adhesive strength of collagen goes far back in time. Gelatine became popular as a food product because of its stabilizing effect, odorless taste, and gelling properties. Furthermore, gelatine has been used in photography, medicine, and pharmacy [73]. As multifunctional and multifarious material, gelatine has found its way into modern science, mostly employed as culture media for microbiological purposes. In 2010, gelatine entered the field of electronics through the demonstration of the first fully biodegradable and biocompatible OFET with hard gelatine as substrate [30]. Hard gelatine has a rather smooth surface with an rms roughness of 30 nm. For electronics fabrication it is important that the roughness of the substrate be minimized because that roughness will be transferred during the fabrication process to all layers above and will ultimately impair the functionality of interfaces between the dielectric and semiconductor and semiconductor and electrode layers.

As shown in Figure 1.19, the additional deposition of a smoothening layer, such as rosolic acid spin coated from ethanol solution, reduced the rms roughness of the hard gelatin down to ~9 nm, which was more amenable for device fabrication and led to improved transistor characteristics exemplified in very low leakage currents not exceeding 1 nA, five orders of magnitude on–off current, and low operating voltage. Besides the use of hard gelatine as substrate, the application of solution-based gelatine as dielectric was investigated by Mao *et al.* [74]. In a follow-up contribution, the group enhanced the dielectric properties of the solution-based gelatine with an additional TTC layer to form a TTC–gelatine bilayer [75]. Figure 1.20 shows the schematic of the corresponding device. The thermally evaporated TTC layer on the spin-coated gelatine film acts as a passivation layer and reduces the hysteresis loop and leakage currents of the p-channel pentacene OFET and the n-channel PTCDI-$C_8$ OFET compared to OFETs having only a

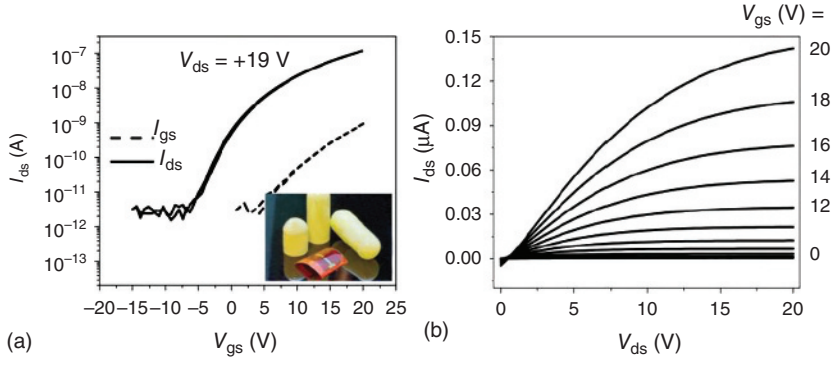


**Figure 1.19** (a) Transfer and (b) output characteristics of OFETs fabricated on hard gelatine capsule. (Irimia-Vladu *et al*. 2010 [30]. Reproduced with permission of John Wiley and Sons.)

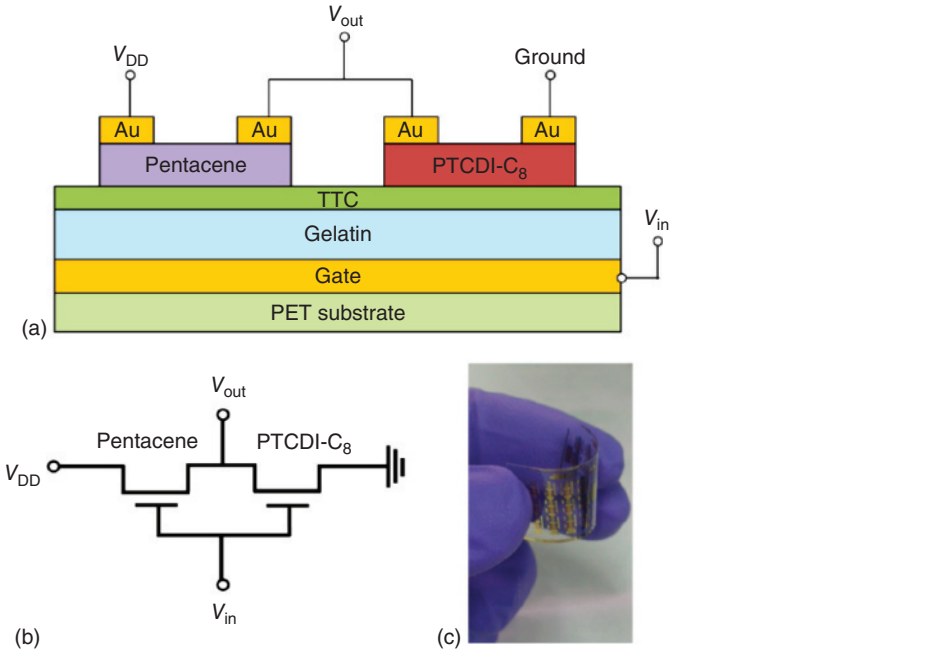


**Figure 1.20** (a) Schematic of the inverter device fabricated on plastic substrate with gelatin as gate dielectric; (b) diagram of the circuit; and (c) photograph of the flexible CMOS inverter. (Mao *et al*. 2015 [75]. Reproduced with permission of Elsevier.)

solution-based gelatine dielectric and no TTC. Another interesting application of gelatine is in the field of polymer composites. The emerging field of degradable bioelectronics and biomedical devices requires materials that have tunable properties such as solubility and degradation over a well-defined period of time. The work of Acar *et al*. [46] demonstrated that gelatine filler, when added to PVA as polymer matrix, can significantly influence the material performance. The biodegradability and nontoxicity of both materials is very well known, which make them ideal candidates for transient electronics [76]. In this respect, the work of Acar *et al*. showed that an increasing amount of gelatine in the PVA–gelatine composite leads to a decreasing solubility of the polymer film and therefore to a controlled dissolution of the layer when employed in electronics fabrication.

Another very interesting approach was the fabrication of an edible supercapacitor made out of food-based components by Wang *et al*. who used gelatine as a packaging material [77]. A schematic structure of the "green" supercapacitor is presented in Figure 1.21.

By employing all edible materials (activated charcoal for the electrodes, Gatorade fluid for the electrolyte, seaweed for the separator membrane, cheese as the segregation layer, gold leaf for collector electrodes, and gelatine as encapsulate), the authors demonstrated the amenability of the design to successfully act as electric source. The edible supercapacitor design was able to support the functionality of a USB camera when connecting in series 5 such fully charged 4 cm × 4 cm square (electrode area) supercapacitors. The series of supercapacitors was able to supply

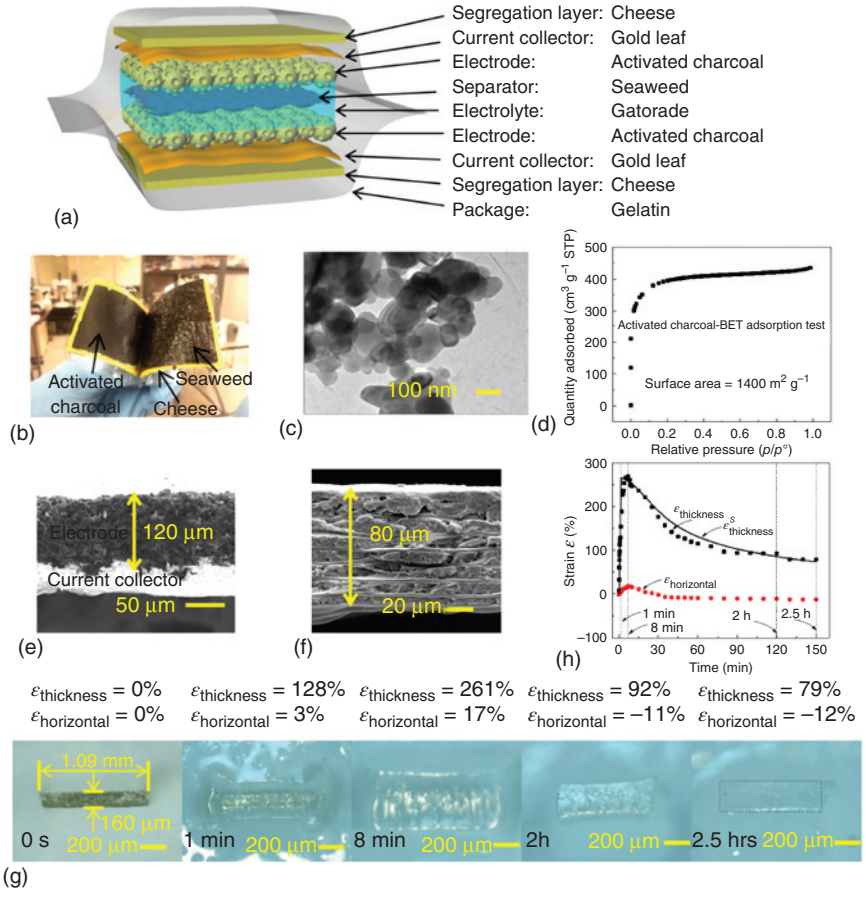


**Figure 1.21** (a) Schematic of the materials employed for the fabrication of edible supercapacitors; (b) photograph of the device; (c) transmission electron microscopy image of the activated charcoal; (d) the employed test, Brunauer–Emmett–Teller, to calculate the surface area of the activated charcoal; (e) scanning electron microscopy image of the cross section of the activated charcoal electrode; (f) cross-section SEM image of the seaweed separator; (g) dissolution test of the gelatine encapsulate; and (h) the time evolutions of the strains showing both experiments and simulations. (Wang *et al*. 2016 [77]. Reproduced with permission of John Wiley and Sons.)

the required 3.3 V necessary to power the camera, which recommends the design for further development of implantable biomedical devices.

From an ecological point of view, gelatine is a non-problematic material. Gelatine is produced from leftovers in meat processing plants that would otherwise be discarded, and therefore it is sustainable. Its composition is a mixture of peptides and proteins produced by partial hydrolysis of collagen extracted from the bones, skin, and connective tissues of animals. It seems reasonable to believe that future electronics development will harvest the high versatility of gelatine imparted by many possibilities of its chemical modification for the achievement of biocompatible stretchable and conformable electronic devices.

## 1.10 Proteins, Peptides, Aminoacids

New developments in science and technology demand sophisticated materials of very high quality. An unusual source of inspiration for electronic materials comes from things we see or touch on a daily routine. One very good example is the work of Chang *et al*. [78] who used albumen, nothing else but the chicken egg white, as gate dielectric in pentacene- and $C_{60}$-based OFETs. The albumen film showed impressive dielectric behavior and surface smoothness, with a measured rms roughness of ~1.5 nm, which made it suitable for OFET device fabrication. Figure 1.22A left frame shows the schematic of the device. The specific capacitance of albumen is 12 nF cm$^{-2}$ with a dielectric constant of 5.3–6.1. Figure 1.22Ba,b shows output and transfer characteristics of a pentacene-based OFET with albumen as gate dielectric. Samples prepared with a $C_{60}$ semiconducting layer show similarly remarkable characteristics. Noticeably, both the n- and the

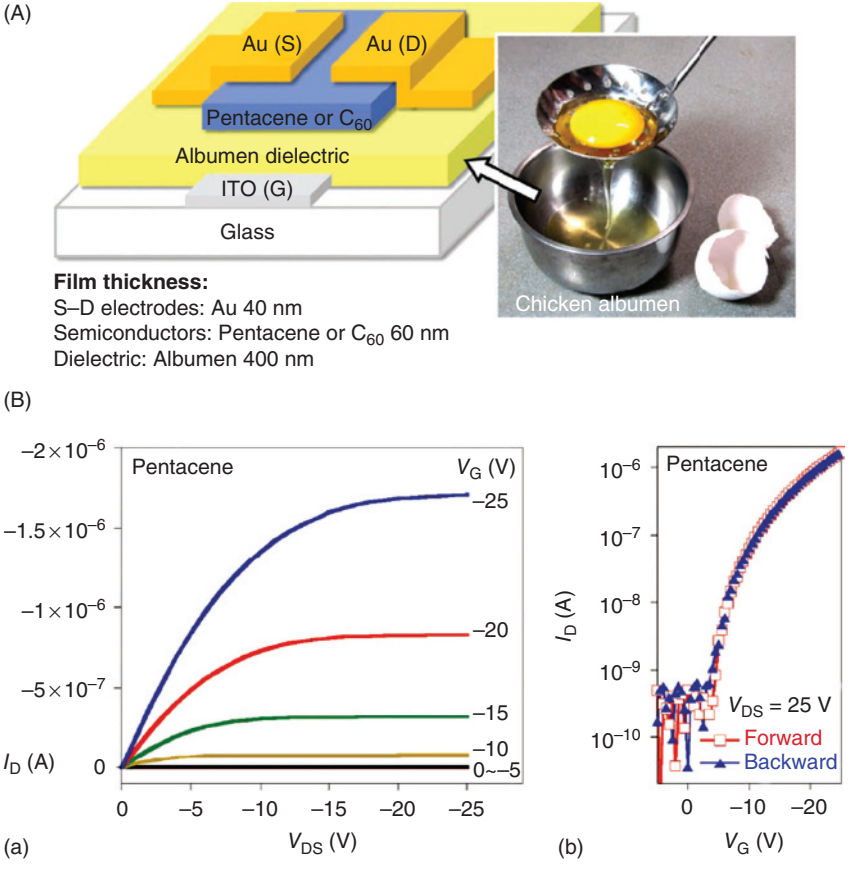


**Figure 1.22** (A) OFET schematic employing cross-linked egg white and pentacene for the organic dielectric semiconductor respectively and (B) transfer and output characteristics for the fabricated devices. (Chang *et al*. 2011 [78]. Reproduced with permission of John Wiley and Sons.)

p-type devices display no obvious hysteresis, credited to the low trap density and smoothness of the dielectric layer.

In a very interesting publication, Wu *et al.* showed that by carefully controlling the level of hydration in egg white layer dielectric, and therefore the proton migration in polypeptide chains under electric field, one can mimic the synaptic activity in brain by using multiple in-plane gates in an indium tin oxide, ITO floating gate with indium zinc oxide, IZO semiconductor field-effect transistor (Figure 1.23Aa) [79]. Figure 1.23Ab shows the transfer curves of the TFT, where the nonvolatile memory effect is shown for various scan rates and ranges of the gate voltage with a maximal hysteresis window of 4 V obtained at 8 V applied $V_{gs}$ voltage. The interesting characteristic of this configuration is that the synaptic device can form a

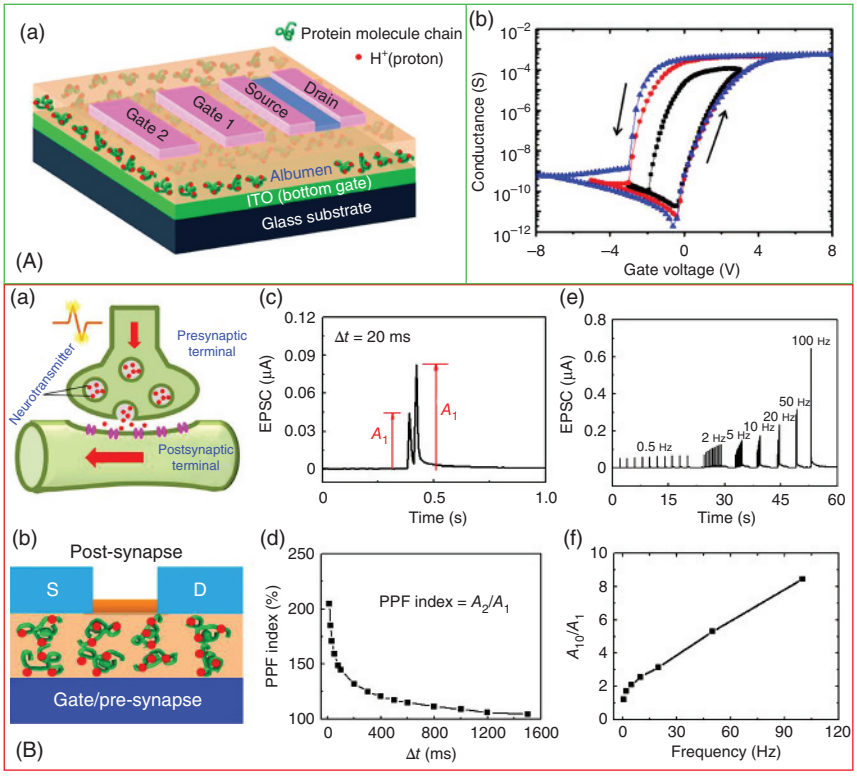


**Figure 1.23** (A) (a) Schematic of the albumen-gated IZO-based synaptic transistor with two in-plane gates used to trigger the current spike formation; (b) recorded nonvolatile memory measurements at various scan rates and voltage ranges; (B) (a,b) schematic of the neuronal synapse and the fabricated TFT device that mimics the biological function; (c–f) various figures of merit of spikes modulation and their recording: (c) a pair of applied presynaptic spikes called paired pulse facilitation (*PPF*) triggering the EPSC under an interspike interval of 20 ms; (d) the PPF index plotted versus interspike interval $\Delta t$; (e) the dynamic filter behavior of the albumen-gated synaptic transistors a function of the stimulus train for various applied frequencies; (f) the EPSC amplitude gain as a function of pulse frequency [79]. (Wu *et al.* 2016, http://www.nature.com/srep/2016/160324/srep23578/full/srep23578.html. Used under CC-BY-4.0 http://creativecommons.org/licenses/by/4.0/.)

connected network with the in-plane gates through strongly lateral electric-double-layer (EDL) coupling, and thus mimic the spike-modulated movement of the neurotransmitters in biological synapses such as in the human brain. In our brain, the most important functions, including learning, signal processing, and memory, are controlled by precise modulation of ion fluxes through neurons and synapses. Neurotransmitters are transported through ion fluxes and can modulate the synapse efficiency by establishing a connection between the presynaptic and postsynaptic neurons (Figure 1.23Ba). The figure of merit of the synaptic strength is the ionic excitatory postsynaptic potential (*EPSP*), which is nothing else but a momentary current caused by the movement of ions into the postsynaptic neuron as a consequence of the presynaptic neuron spike. In this ingenuous representation of

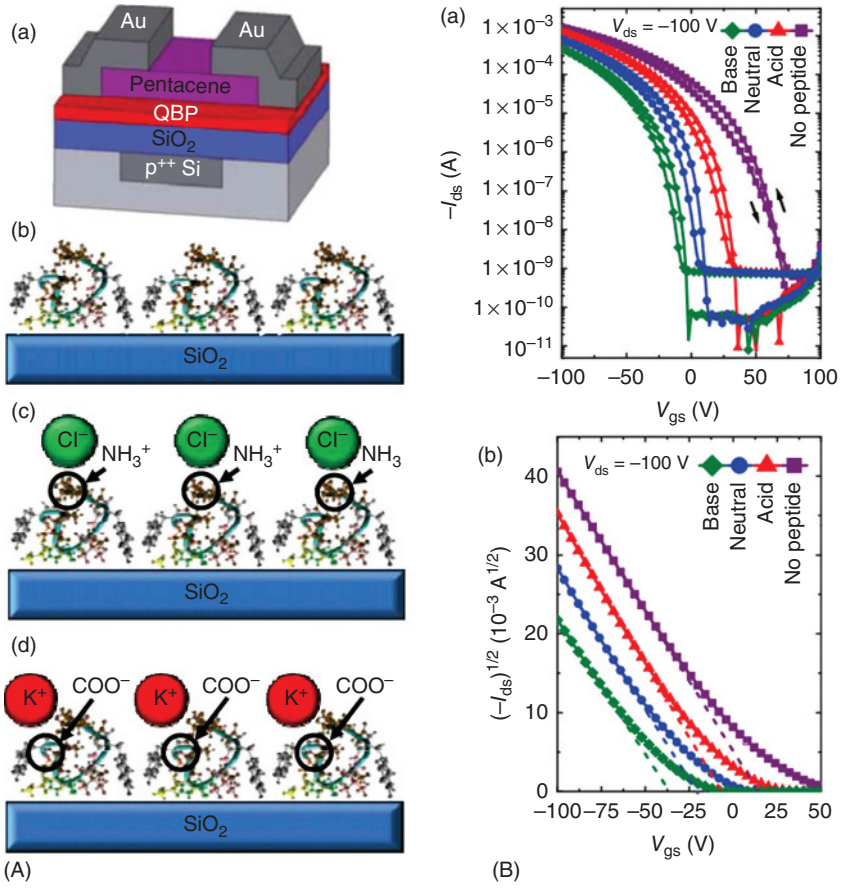


**Figure 1.24** (A) (a) Schematic of a peptide-modified thin-film transistor; studied cases of peptide assembly in: water (b) where no ions are present to pair with peptide termini; in acidic solution (c) where, the N-termini of the peptide pair with chloride ions to produce a dipole pointing away from the substrate surface; and in basic solution (d) where the C-termini pair with potassium ions to produce a dipole pointing toward the substrate surface. (B) Transfer characteristics of the device showing the controllable shift of the threshold voltage. (Dezieck *et al*. 2010 [80]. Reproduced with permission of AIP Publishing.)

an electronic circuit that mimics biological actions, the ITO bottom-gate electrode and IZO source/drain electrodes containing channel layer are nothing but the presynaptic and postsynaptic terminals, respectively; the albumen film and its constituent ions (protons) are regarded as the synaptic fork and neurotransmitters respectively; the channel current ($I_{ds}$) is regarded as the excitatory postsynaptic current (*EPSC*), which is considered here instead of the potential (EPSP) to demonstrate the existence of the presynaptic spike (Figure 1.23Bb). It is in fact this presynaptic spike supplied by the gate electrodes G1 and/or G2 that triggers the proton transport within the albumen and consequently the modulation of the channel current.

An OFET has parameters that can be tuned in order to improve device performance. One such important factor is the threshold voltage ($V_T$). Dezieck *et al.* found a way to control $V_T$ in organic thin-film transistors with a dielectric layer modified by a genetically engineered polypeptide [80]. Controlling $V_T$ can yield higher circuit performance and lower power consumption in electronics. In their work they used a genetically engineered peptide for inorganics (*GEPI*s), basically a quartz binding polypeptide (*QBP*) of a specific amino acid sequence, which preferentially and strongly binds to silicon dioxide ($SiO_2$). The authors prepared different solutions of aqueous QBP with varying pHs to modify the organic semiconductor–$SiO_2$ interface in an OTFT and tune the threshold voltage through the control of the peptide assembling conditions as shown in Figure 1.24. OTFTs modified with QBP were assembled on $SiO_2$ under basic, neutral, and acidic conditions with and without peptide. A positive shift in $V_T$ was observed when QBP was assembled in acidic conditions, whereas a negative shift in $V_T$ was observed when QBP was assembled in basic solutions.

## 1.11 Natural and Nature-Inspired Semiconductors

There are a number of molecular materials of natural origin that are intrinsically semiconducting and can be used as active components in (opto) electronic devices. Some of the compounds responsible for photosynthesis, for example, are chromophores with extensive conjugation, such as porphyrins and polyenes. Their chemical structures closely resemble the ones of many of the synthetic, conjugated semiconductors. Tang and Albrecht processed thin films of chlorophyll *a* to produce sandwich-type photovoltaic diodes in 1975, representing a seminal example of harnessing a naturally available semiconductor in a solid-state device [81]. Since then, chlorophyll was used in solid-state photovoltaic diodes; however, low power conversion efficiency and poor charge transport, and in particular operational stability were major problems of those pioneering devices. In the early 1990s, Moses *et al.* explored the consequences of the similarity of beta-carotene with the well-known conducting polymer polyacetylene [82]. Like polyacetylene, carotene was found by the authors to have spinless solitons upon doping, which indicated its suitability for applications in organic electronics. Beta-carotene semiconductor was solution processed from chloroform solution to make films suitable for thin-film transistors, with hole mobility of $1 \times 10^{-4}\,cm^2\,V^{-1}\,s^{-1}$ and also explored in bulk heterojunction organic photovoltaic

devices, nevertheless with modest performance [83, 84]. As in the case of chlorophyll *a*, operational stability was a major problem, as beta-carotene rapidly oxidized when exposed to ambient oxygen. Evolution has not endowed these natural conjugated chromophores with long-term stability. Indeed, the metabolism of living systems continuously regenerates these molecules.

Over the course of human history, people were surrounded by natural colors, but found that very few of them could be used to make stable pigments or dyes. Through a long selection process, a few natural-origin chromophores emerged as suitable colorants for artistic purposes [85, 86]. Nearly all of the organic materials utilized as dyes and pigments prominently feature both intra- and intermolecular hydrogen bonding, which leads to the desired coloristic properties and most importantly promotes stability. These molecules are relatively small one or two condensed ring structures with carbonyl and often amine functional groups, which are sometimes colorless when dissolved in true solutions [87–89]. Hydrogen bonding mediates aggregation and crystallization and leads to marked bathochromic shifts in absorption upon aggregation. In this way, small molecules that are intrinsically stable assemble into crystals with a strong UV–vis absorption and additional stability afforded by high crystal lattice energy. It is this family of so-called hydrogen-bonded pigments that holds promise as a natural source of stable semiconductors. Indigo is one of the most well-known natural-origin dyes used throughout history, with different derivatives obtainable from plant and animal sources (Figure 1.25a,b) [91, 92]. Owing to its high crystal lattice energy, indigo is not soluble in its neutral form; therefore, fabric dyeing technique relies first on a chemical reduction step to obtain a water-soluble leucoindigo (Figure 1.25c).

After allowing leucoindigo to penetrate into the fibers, the textile is withdrawn into air where oxygen oxidizes the leucoindigo back into the insoluble neutral blue-colored form, giving a permanent coloration to the fabric. This process of so-called vat dyeing highlights also the versatile and reversible redox states of these types of molecules. Besides being known to be nontoxic (i.e., indigo carmine, the sodium sulfate salt of indigo is an approved food colorant), indigo is the single most widely produced industrial dyestuff, with 20 000 tons per year used only for the dyeing of blue denim fabric [93]. Reproducing the vat dyeing technique of indigo processibility for organic electronics fabrication is not desirable because of the inherent ionic content of the deposited film. Interestingly though, indigo sublimes and can be scrupulously cleaned through train sublimation technique; thin films of pure indigo can be therefore deposited via vacuum sublimation at temperatures below 300 °C in high vacuum chambers. Mainly due to its stability (indigo has reasonably good fading resistance against UV radiation) and easy processibility, indigo was identified as a promising semiconducting material for organic electronics. Irimia-Vladu *et al.* reported in 2012 that indigo was an ambipolar semiconductor with balanced electron and hole mobilities of $1 \times 10^{-2}\,cm^2\,V^{-1}\,s^{-1}$ and good stability against degradation. In their seminal work, the authors vacuum-processed an indigo semiconductor using TTC as a gate dielectric material (discussed in Section 1.6) and shellac resin as a substrate (Section 1.8) [72]. Their effort represented the first thin-film transistor fabricated exclusively from natural-origin materials (Figure 1.26).

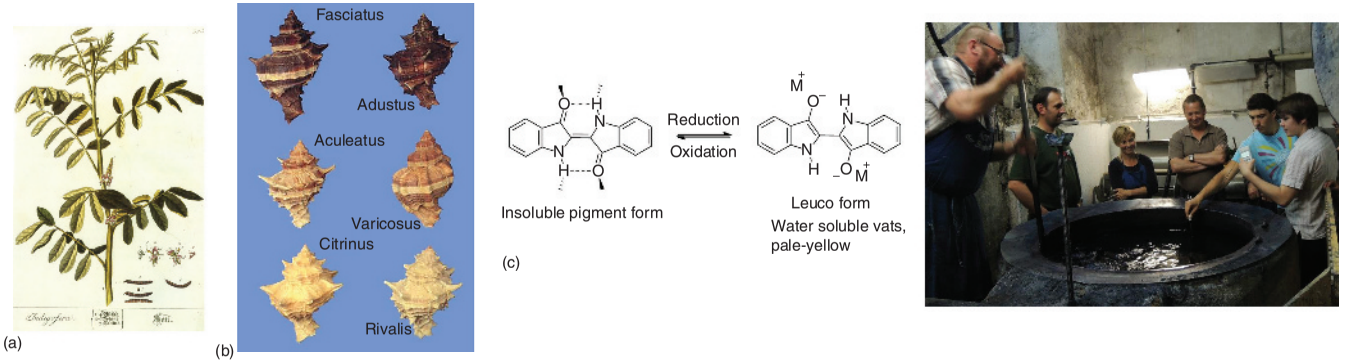


**Figure 1.25** (a) Image of *Indigofera tinctoria*, the tropical source of indigo; (b) various snails from the Muricidae and Thaisidae families represented the natural source of Tyrian purple dyes; (c) the chemistry of vat dyeing involving the reduction of indigos to produce an aqueous solution of $Indigo^{-1}$ (indigo radical), and $indigo^{-2}$ (fully reduced, known as leuco or "white" indigo) with various metal counterions, most typically $K^+$ and $Na^+$. The photo shows two of the authors visiting a traditional indigo vat dyeing facility in Bad Leonfelden, Austria (EDG-right, white shirt, and MIV-left, green shirt). (Glowacki *et al*. 2013 [90]. Reproduced with permission of John Wiley and Sons.)

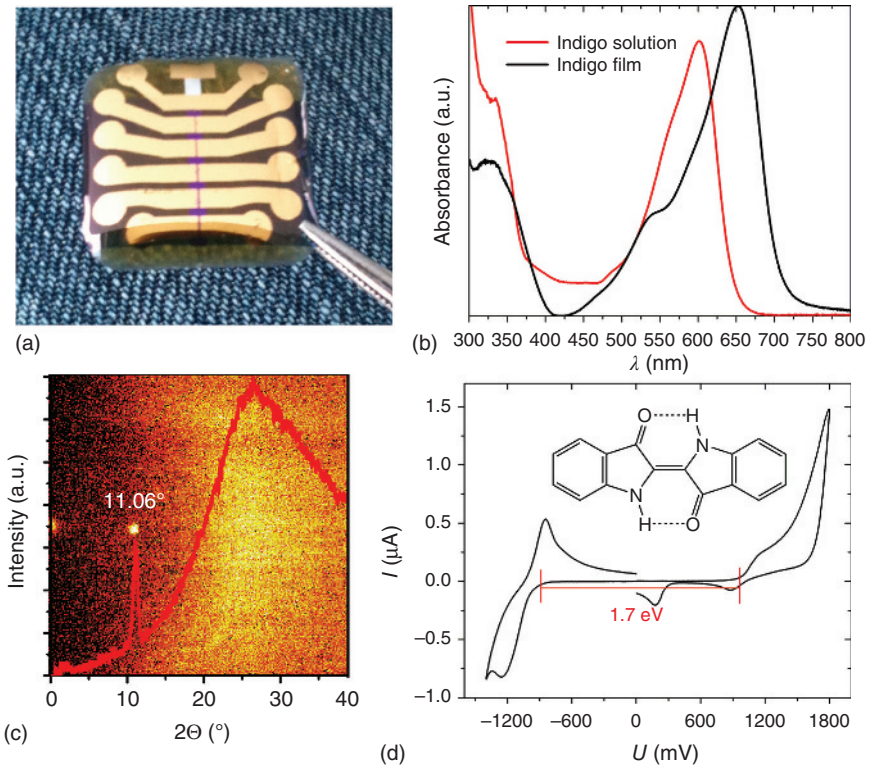


**Figure 1.26** Indigo field-effect transistors: (a) Photograph of ambipolar indigo transistors fabricated on shellac with aluminum oxide-tetratetracontane dielectric and gold source and drain electrodes; (b) optical absorption spectra of an indigo solution in chloroform (red) and of a thin evaporated indigo film (black), showing a bathochromic shift of absorbance onset of ~100 nm in the indigo film in comparison to the solution; (c) XRD of an indigo thin film grown by thermal evaporation on tetratetracontane; and (d) cyclic voltammetry scans of indigo films using ITO|indigo as the working electrode. The quasireversible two electron exchange electrochemistry correctly predicts the possibility of ambipolar transport in indigo molecule. (Irimia-Vladu *et al*. 2012 [72]. Reproduced with permission of John Wiley and Sons.)

Tyrian purple, 6,6′-dibromoindigo, a natural pigment extracted historically from Mediterranean Sea snails (Figure 1.25b) was also found to be an ambipolar semiconductor in transistors and was used to fabricate near-infrared-absorbing heterojunction diodes with silicon [94–96]. van der Waals interactions between bromine atoms promote enhanced π–π stacking in Tyrian purple, leading to balanced electron and hole mobilities in the range of $0.4\,cm^2\,V^{-1}\,s^{-1}$ [95]. The crystal structures of both molecules helps explaining the observed charge transport behavior (Figure 1.27). While intermolecular hydrogen bonds cause the indigo molecules to arrange into hydrogen-bonded chains, these chains π–π stack along the axis perpendicular to the hydrogen-bonding axis. It was found in various studies that the orientation of the growing crystals with respect to the substrate has a profound effect on the occurrence of charge transport [97, 98]. The π–π stacking axis, for instance, must be parallel to the gate dielectric in order to

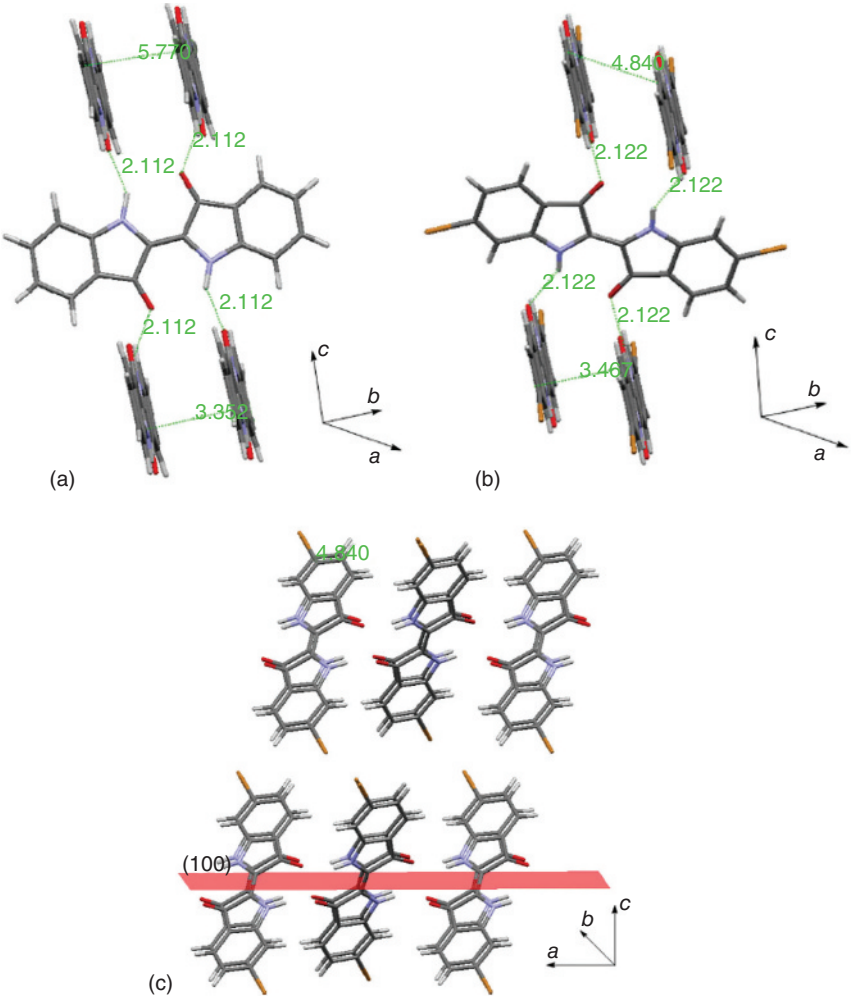


**Figure 1.27** (a) Indigo crystal structure showing the interplanar spacing along the b-axis between two stacked indigo molecules (3.352 Å) and the interatomic distances between two equivalent positions (5.77 Å); (b) Tyrian purple (6,6′-dibromoindigo) crystal structure, having an interplanar spacing of 3.46 Å, and an interatomic distance between two equivalent positions of 4.84 Å; and (c) Tyrian purple view along the b-axis (stacking direction). The only visible peaks of Tyrian purple when grown on hydrophobic (low surface energy) gate dielectrics are [100] and other [*h*00]. This kind of stacking parallel to the substrate is ideal for obtaining charge transport between source and drain electrodes in OFET design. (Glowacki *et al*. 2013 [90]. Reproduced with permission of John Wiley and Sons.)

obtain good charge mobility in thin-film transistor geometry [72, 90, 99]. Several successful examples of chemically modified indigos, some with extended π-conjugation, have been shown in organic transistor applications [100, 101]. The substitution of indigo can alter packing and crystallization and lead to large changes in mobility. Moreover, the anisotropic nature of transport, wherein one crystallographic axis dominates in contributing to charge transport, leads to vast

differences in observed charge transport behavior, depending on substrate properties and deposition conditions.

The term hydrogen-bonded pigments, although accurate in describing the naturally derived materials discussed above, historically originated with respect to organic-molecular solid-state colorants of synthetic origin [102]. This term entered the field of industrial organic pigments since the introduction of hydrogen-bonded groups was recognized for promoting stability and allowing control on aggregation behavior (i.e., polymorphism and crystallochromy), which ultimately led to obtaining the desired colors [103]. Industrial pigment chemists and technologists, however, normally categorize colorants by their chemical "family" – for example, azo compounds, phthalocyanines, and quinacridones. Many compounds from these families can be considered as belonging to the hydrogen-bonded pigment class [104]. Most of these materials are generally considered nontoxic; due to their intense lack of solubility they are simply not bioavailable, but only synthetically produced. Only a few of these materials have been studied in detail with results published in scientific literature with respect to their electro-optical properties or even biodegradation amenabilities. A much larger body of knowledge exists, however, in the realm of patents and technological and engineering bulletins, but the reported properties of those dyes and pigments are restricted to their practical colorant properties. Some pigments have been studied for their toxicological and environmental impact, in the context of their deployment on a large scale in consumer products such as outdoor paint formulations, printing inks, various cosmetic formulations as well as tattoos [105].

One of the most prominent synthetic hydrogen-bonded pigments, produced on an industrial scale, is quinacridone [106]. Quinacridone is best known as the magenta pigment for printing inks, but is also found in paints and cosmetic products [104]. Quinacridone was explored as an active material for solar cells [107] and thin-film transistors, achieving hole mobilities of $0.1\,cm^2V^{-1}s^{-1}$, with about one order of magnitude lower electron mobility [55]. Quinacridone, however, is characterized by excellent operation stability in devices operated in ambient air without encapsulation [55]. Another interesting hydrogen-bonded molecule with an outstanding stability is epindolidione, which is nothing else but a structural isomer of indigo. Different than quinacridone, epindolidione does not have a straight forward synthetic route, but alternatively can be synthesized by a high-temperature solid-state thermal rearrangement of indigo in high vacuum [55, 108]. Epindolidione also shows ambipolar charge transport as its isomer indigo, but outplays indigo in performance, affording hole mobilities greater than $1\,cm^2V^{-1}s^{-1}$ [109]. Quinacridone and epindolidione are luminescent both in dilute solution and in solid state, whereas indigo is not, because of the ultrafast photoinduced proton transfer that leads to very efficient nonradiative deactivation of its excited state (Figure 1.28). Epindolidione and quinacridone demonstrate various excimeric and defect-luminescence behavior in solid state, apparently due to the intermolecular hydrogen-bonding interaction, which contributes to efficient delocalization of excited states between neighboring molecules [109, 110]. For bioelectronics applications, epindolidione and quinacridone have promising properties mainly because of their stability and amenability for further functionalization. Glowacki *et al.* showed that thin-film transistors with

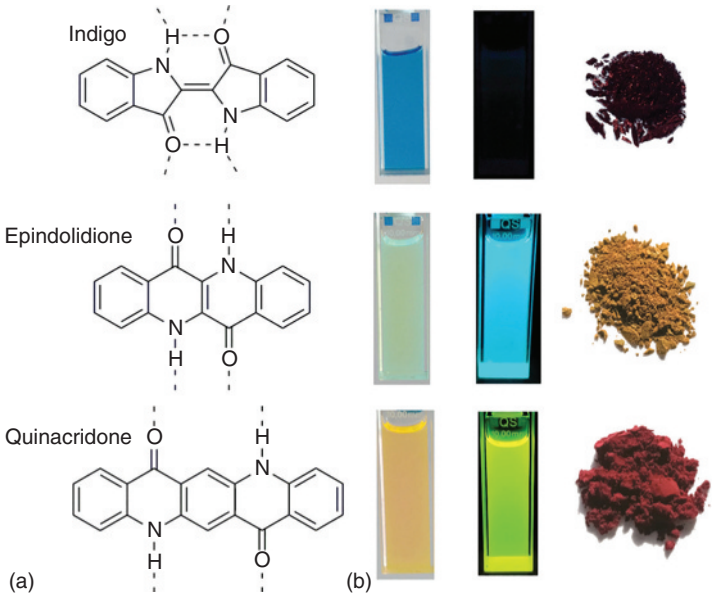


**Figure 1.28** (a) Molecular structures of indigo, its isomer epindolidione, and quinacridone, with dashed lines indicating hydrogen bonding; (b) solutions of 0.1 mM of each material in dimethyl sulfoxide (*DMSO*), with photoluminescence excitation at 365 nm. Epindolidione and quinacridone are highly emissive, while indigo shows very low luminescence quantum yield. On the right, the powders of the three pigments are shown, where the bathochromically shifted absorption and tinctorial strength are visible compared to their respective solution. (Glowacki *et al*. 2015 [109]. Reproduced with permission of John Wiley and Sons.)

epindolidione semiconductor could be fabricated to operate in a low-voltage window by using ultrathin alumina dielectric layers (Figure 1.29) [109]. Such devices operated stably in a pH range from 3 to 10 over hundreds of cycles in direct contact with electrolytic solutions, without the need of passivation. Both epindolidione and quinacridone can be bioconjugated easily via nucleophilic attack of the amine functional groups on *N*-succinimidyl esters, which can in turn be used as linkers to covalently attach biomolecules of interest to the surface of the hydrogen-bonded semiconductor (Figure 1.30) [111]. The authors demonstrated successful linking of a photosynthetic reaction center protein to the semiconductor epindolidione and quinacridone molecules, with confirmed preservation of both protein and semiconductor functions after bridging. The outstanding stability of epindolidione and quinacridone in aqueous solutions is further underscored in their photoelectrocatalytic performance in reducing oxygen selectively to hydrogen peroxide, which represents a valuable molecule for a plethora of biological contexts. Jakešová *et al*. showed that these photocathodic reactions can proceed in a pH range from 1 to 12 over at least 4 days of continuous operation, with some experiments recording more than 2 weeks of stable operation at pH 1 (Figure 1.31) [112]. The unique photocatalytic ability of these two pigments is enabled by the combination of a high-lying (and thus highly-reductive) LUMO level with their inherent stability – normally organic

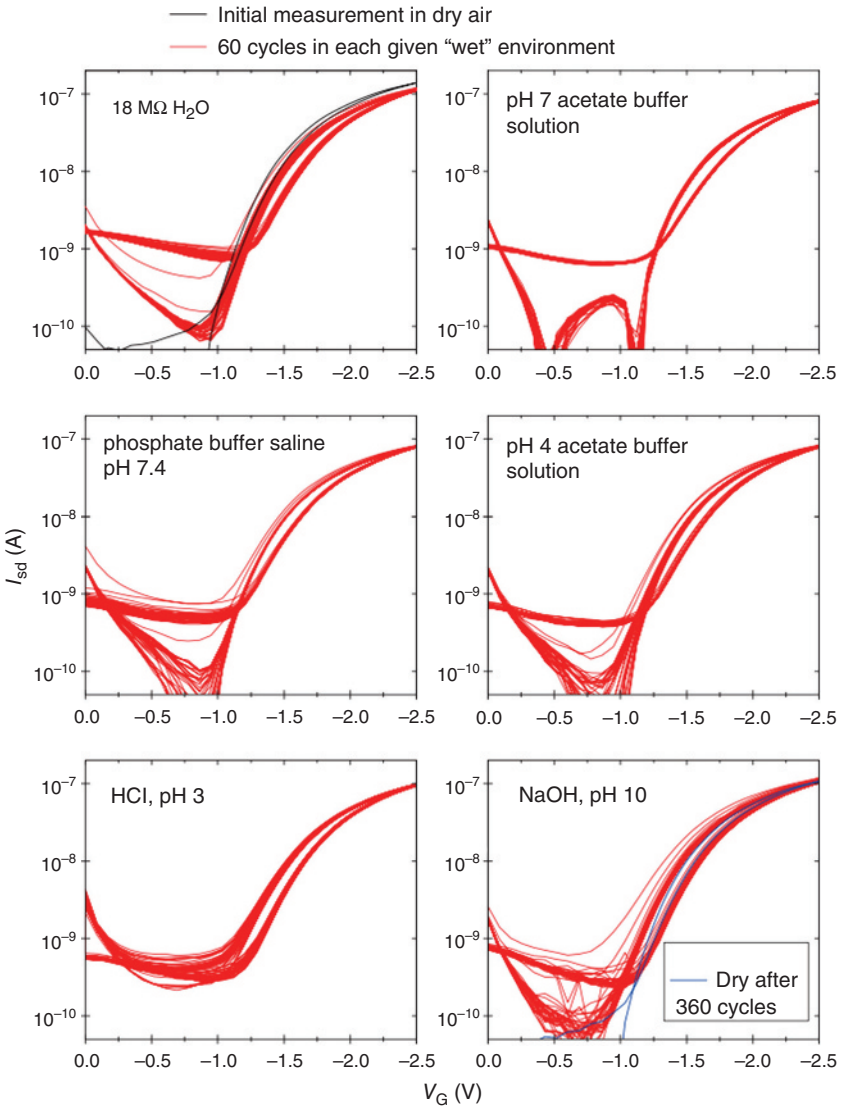


**Figure 1.29** Low-voltage operating OFETs with epindolidione semiconductor fabricated on thin aluminum oxide dielectric. The devices were measured with an applied source–drain voltage, $V_{ds} = -0.5$ V in air (black curve) followed by 360 cycles in six different aqueous environments, with 60 cycles carried out in each medium (red curves). Samples were rinsed with deionized water when moving from one electrolyte to another. (Glowacki *et al*. 2015 [109]. Reproduced with permission of John Wiley and Sons.)

semiconductors with such high-lying states are unstable in oxygenated or water-containing environments. The stability of these pigments, enabling catalysis, represents a new direction for organic semiconductors research, and the recent progress of the use of quinacridone in organic semiconducting devices has been recently reviewed [113].

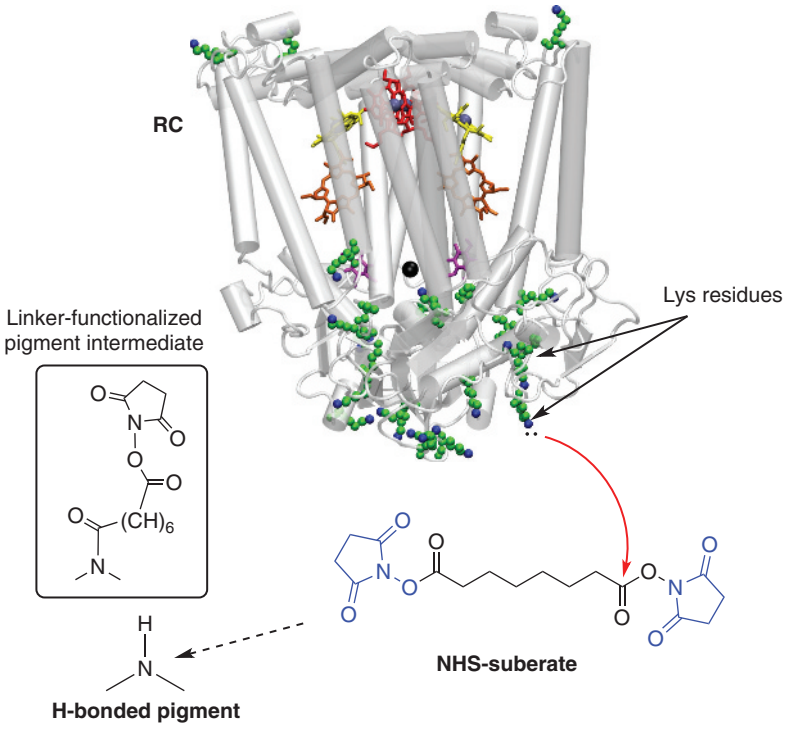


**Figure 1.30** The proposed bioconjugation procedure of the *Rhodobacter sphaeroides* photosynthetic reaction center (*RC*) to hydrogen-bonded pigments (quinacridone and epindolidione) using the disuccinimidyl suberate linker. The *N*-succinimidyl ester (NHS) function on the linker is introduced in order to selectively address the amine nucleophiles on the pigments. The NHS groups that are cleaved during the bioconjugation process are shown in blue. The crystal structure of the RC with its 22 lysine residues available for conjugation is shown at the top of the figure [111]. (Glowacki *et al*. 2015, http://pubs.rsc.org/en/Content/ArticleLanding/2015/TC/c5tc00556f#!divAbstract. Used under CC-BY-3.0 http://creativecommons.org/licenses/by/3.0/.)

Apart from indigos and quinacridones, flavanthrone and indanthrone pigments (synthetic derivatives of anthraquinones) are also produced in large scale and widely employed as dyestuffs and cosmetic colorants. They have also shown promising performance in organic transistor devices and light-emitting diodes, as demonstrated through several publications [83, 114, 115].

Many of the above-mentioned compounds and classes of compounds (either hydrogen bonded or not) have as a common feature the high crystal lattice energy that makes their processibility difficult via solution and sometimes even via vacuum sublimation routes. Indeed, some dyes and pigment molecules cannot be processed in their purest form (e.g., vat blue 20, vat green 8 and its isomers, and many others anthraquinones), and can be used only as dispersions afforded by the presence of a specific surfactant. All hydrogen-bonded pigments are characterized in fact by very low solubility in organic or aqueous solvents. Typically, stable solutions can only be obtained in relatively low concentrations on the order of 0.1–0.2 mM in highly polar hydrogen-bond-forming solvents such as dimethyl sulfoxide or

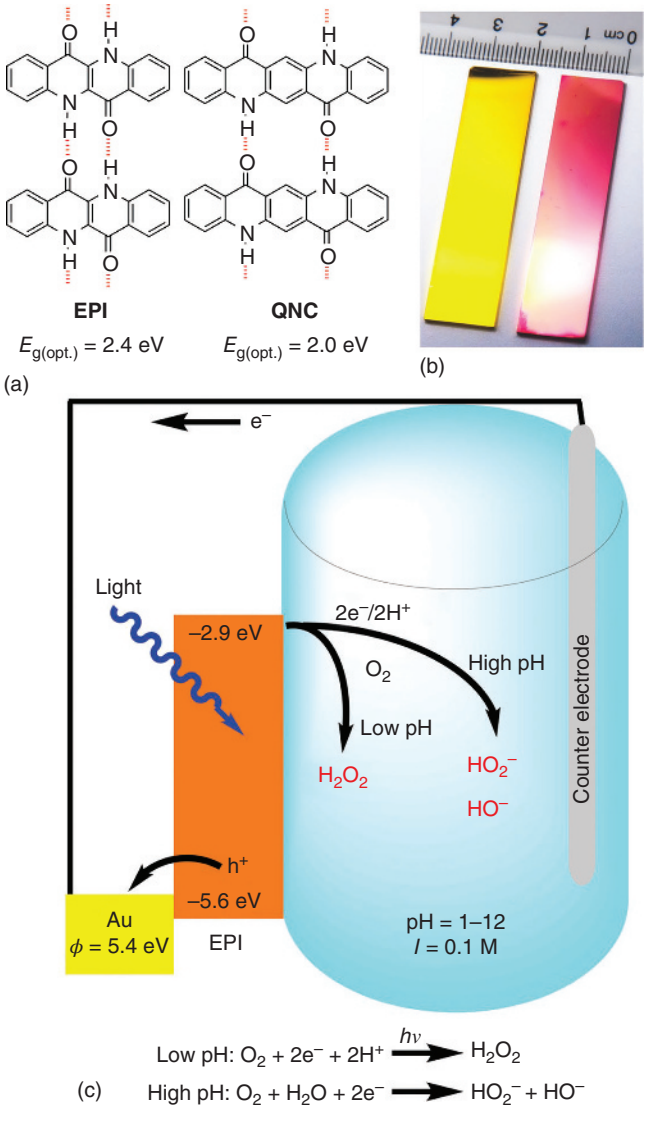


**Figure 1.31** (a) Molecular structure of hydrogen-bonded pigment semiconductors epindolidione (*EPI*) and quinacridone (*QNC*) with the measured optical band gap at the bottom; (b) EPI (left) and QNC (right) photoelectrodes, consisting of thin polycrystalline films vacuum deposited on gold coated glass slides; and (c) schematic of the photoelectrochemical measurement setup with EPI semiconductor electrode. The measurement involved aqueous electrolytes in the pH range 1–12. Oxygen reduction reactions at low and high pH levels occur via the equations shown. (Jakešová *et al*. 2016 [112]. Reproduced with permission of John Wiley and Sons.)

dimethylformamide. This property impedes any reliable solution processibility of devices and also limits the range of chemical reactions that can be used to modify the fundamental pigment chromophores. Substituting the pigment-forming molecules with large alkyl chains can impart some solubility in organic solvents, yet

hydrogen bonding leads to rapid aggregation. An alternative strategy is transient substitution of the hydrogen-bonding functional groups with a protecting group that can be cleaved in a controlled way. Zambounis *et al.* reported the so-called latent pigment approach by attaching a *tert*butoxy carbonyl functional group (*tBOC*) to the amine function of the pigments using the highly reactive dianhydride of *t*BOC [116]. This design effectively blocks any hydrogen-bond formation and leads to dyes with very high solubilities in typical organic solvents. The *t*BOC group can be irreversibly degraded by heat treatment or acid vapor exposure, leading to gaseous byproducts. Zambounis *et al.* used this technique for technical coloristic purposes, whereby a latent pigment could be processed and then deprotected at a specific processing step. This procedure can be used to disperse pigment particles uniformly in host polymer films, for example [117]. This method can be used for the solution processing of indigos and quinacridones, and can yield derivatives that are soluble and therefore amenable to multistep synthetic modification [118, 119]. It can also be used to produce blends of indigos with semiconducting polymers such as polythiophenes or to synthesize controlled colloids of nano- and microcrystals. When the *t*BOC protected form of a pigment is dissolved and then chemically or thermally deprotected in the presence of various ligands, colloidal crystals can be grown with tunable size and shape (Figure 1.32). This procedure

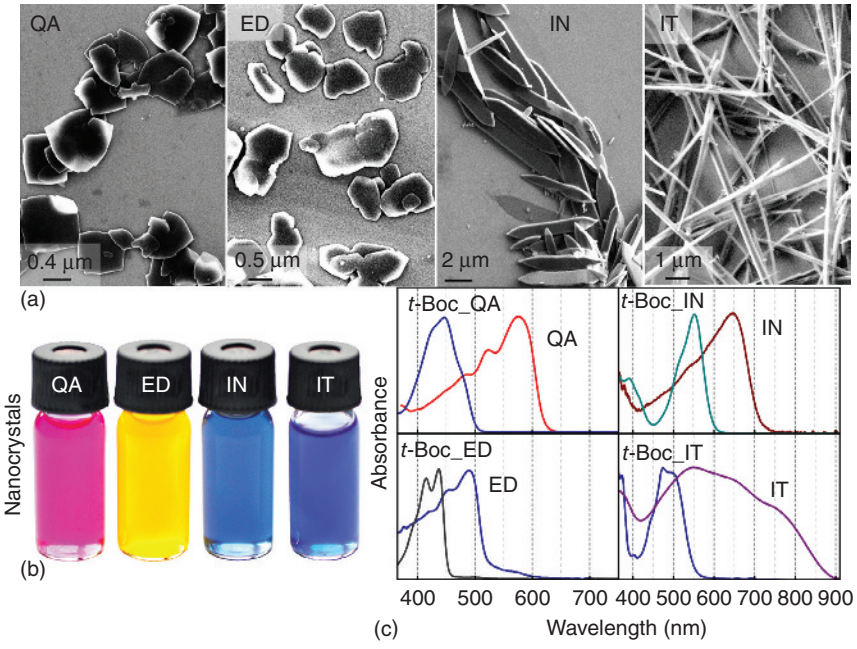


**Figure 1.32** (a) Electron micrographs of the colloidal micro-nanocrystals of organic pigments on a Si substrate (*QA*, quinacridone; *ED*, epindolidione; *IN*, indigo; *IT*, indanthrene). The pigments were synthesized by cleavage of the thermolabile *t*BOC protection groups from the latent pigment precursors; (b) image of the vials containing the colloidal dispersions; and (c) absorbance spectra of the latent pigment precursors and the synthesized organic pigment micronanostructures [120]. (Sytnyk *et al.* 2014, https://www.ncbi.nlm.nih.gov/pmc/articles/PMC4277760/. Used under CC-BY-4.0 http://creativecommons.org/licenses/by/4.0/.)

yields semiconducting crystals that can be solution processed and used directly in field-effect transistors or photodiodes [120].

The hydrogen-bonded pigment class of materials holds promise for sustainable electronics since the materials are robust and multifunctional and many are well-developed industrially, providing low cost with proven stability. Application of these materials in organic optoelectronics offers motivation for synthetic chemists to again focus their attention on this "old" materials class, and it is likely that research in functional materials based on hydrogen-bonded pigments will expand in the future.

## 1.12 Perspectives

A decade ago, the vision of green and sustainable electronics was not more than pie in the sky, with hesitant approaches toward biodegradable and even edible electronics. Initially seen as an exotic category of cross-disciplinary materials science, "green" electronics became a distinct and booming research area. A wealth of nature-inspired and natural substrates, dielectrics, and semiconductors is now available, useful in support structures and thin-film forms for electronic and optoelectronic devices. Nevertheless, there is still a long way to go until we can dream of a technological era with responsible handling of materials and resources. There are ample opportunities for research, ranging from the identification of sufficiently stable natural materials employable for device design, development, and optimization to the fabrication of prototypes close to commercialization. In the end, we may have a pluripotent platform of lasting technologies for electronics and photonics, changing the way we perceive electronic and photonic systems, with applications spanning smart appliances, sports, healthcare, and well-being.

## References


1 Rogers, J.A., Someya, T., and Huang, Y. (2010) Materials and mechanics for stretchable electronics. *Science*, **327** (5973), 1603–1607.

2 Wagner, S. and Bauer, S. (2012) Materials for stretchable electronics. *MRS Bull.*, **37** (03), 207–213.

3 Bauer, S., Bauer-Gogonea, S., Graz, I., Kaltenbrunner, M., Keplinger, C., and Schwödiauer, R. (2014) 25th Anniversary article: a soft future: from robots and sensor skin to energy harvesters. *Adv. Mater.*, **26** (1), 149–162.

4 Chortos, A., Liu, J., and Bao, Z. (2016) Pursuing prosthetic electronic skin. *Nat. Mater.*, **15**, 937–950.

5 Rogers, J. and Balooch, G. (2016) A restorative synthetic skin. *Nat. Mater.*, **15**, 828–829.

6 Kim, D.-H., Lu, N., Ma, R., Kim, Y.-S., Kim, R.-H., Wang, S., Wu, J., Won, S.M., Tao, H., Islam, A., Yu, K.J., Kim, T., Chowdhury, R., Ying, M., Xu, L., Li, M., Chung, H.-J., Keum, H., McCormick, M., Liu, P., Zhang, Y.-W., Omenetto, F.G., Huang, Y., Coleman, T., and Rogers, J.A. (2011) Epidermal electronics. *Science*, **333**, 838–843.

7 Kim, Y.J., Chun, S.E., Whitacre, J., and Bettinger, C.J. (2013) Self-deployable current sources fabricated from edible materials. *J. Mater. Chem. B*, **1** (31), 3781–3788.

8 Norton, J.S., Leeb, D.S., Lee, J.W., Lee, W., Kwon, O., Won, P., Jung, S.-Y., Cheng, H., Jeong, J.-W., Akce, A., Umunna, S., Nad, I., Kwon, Y.H., Wang, X.-Q., Liu, Z.J., Paik, U., Huang, Y., Bretl, T., Yeo, W.-H., and Rogers, J.A. (2015) Soft, curved electrode systems capable of integration on the auricle as a persistent brain-computer interface. *Proc. Natl. Acad. Sci. U.S.A.*, **112** (13), 3920–3925.

9 Tao, H., Hwang, S.-W., Marelli, B., An, B., Moreau, J.E., Yang, M., Brenckle, M.A., Kim, S., Kaplan, D.L., Rogers, J.A., and Omenetto, F.G. (2014) Silk-based resorbable electronic devices for remotely controlled therapy and in vivo infection abatement. *Proc. Natl. Acad. Sci. U.S.A.*, **111** (49), 17385–17389.

10 2014) *The Global e-waste Monitor 2014: Quantities, Flows and Resources*, United Nations University, Institute for Advanced Study on Sustainability, pp. 1–80.

11 Kang, S.-K., Murphy, R.K.J., Hwang, S.-W., Lee, S.M., Harburg, D.V., Krueger, N.A., Shin, J., Gamble, P., Cheng, H., Yu, S., Liu, Z., McCall, J.G., Stephen, M., Ying, H., Kim, J., Park, G., Webb, R.C., Lee, C.H., Chung, S., Wie, D.S., Gujar, A.D., Vemulapalli, B., Kim, A.H., Lee, K.-M., Cheng, J., Huang, Y., Lee, S.H., Braun, P.V., Ray, W.Z., and Rogers, J.A. (2016) Bioresorbable silicon electronic sensors for the brain. *Nature*, **530**, 71–76.

12 Irimia-Vladu, M. (2014) Green electronics: biocompatible and biodegradable materials and devices for sustainable future. *Chem. Soc. Rev.*, **43**, 588–610.

13 Tobjörk, D. and Österbacka, R. (2011) Paper electronics. *Adv. Mater.*, **23**, 1935–1961.

14 Martins, R., Nathan, A., Barros, R., Pereira, L., Barquinha, P., Correia, N., Costa, R., Ahnood, A., Ferreira, I., and Fortunato, E. (2011) Complementary metal oxide semiconductor technology with and on paper. *Adv. Mater.*, **23**, 4491–4496.

15 Pettersson, F., Österbacka, R., Koskela, J., Kilpelä, A., Remonen, T., Zhang, Y., Inkinen, S., Wilén, C.-E., Bollström, R., Toivakka, M., Määttänen, A., Ihalainen, P., and Peltonen, J. (2014) Ion-modulated transistors on paper using phase-separated semiconductor/insulator blends. *MRS Commun.*, **4**, 51–55.

16 Pettersson, F., Adekanye, D., and Österbacka, R. (2015) Stability of environmentally friendly paper electronic devices. *Phys. Status Solidi A*, **212**, 2696–2701.

17 Barr, M.C., Rowehl, J.A., Lunt, R.R., Xu, J., Wang, A., Boyce, C.M., Im, S.G., Bulovic´, V., and Gleason, K.K. (2011) Direct monolithic integration of organic photovoltaic circuits on unmodified paper. *Adv. Mater.*, **23**, 3500–3505.

18 Leonat, L., White, M., Glowacki, E., Scharber, M., Zillger, T., Rühling, J., Hübler, A., and Sariciftci, S.N. (2014) 4% efficient polymer solar cells on paper substrates. *J. Phys. Chem. C*, **118**, 16813–16817.

19 Fujisaki, Y., Koga, H., Nakajima, Y., Nakata, M., Tsuji, H., Yamamoto, T., Kurita, T., Nogi, M., and Shimidzu, N. (2014) Transparent nanopaper-based flexible organic thin-film transistor array. *Adv. Funct. Mater.*, **24**, 1657–1663.

20 Zschieschang, U., Yamamoto, T., Takimiya, K., Kuwabara, H., Ikeda, M., Sekitani, T., Someya, T., and Klauk, H. (2011) Organic Electronics on Banknotes. *Adv. Mater.*, **23**, 654–658.

21 Kim, S., Ko, H., Lee, C., Kim, M.K., Kim, K.S., Lee, Y.-H., Shin, K., and Cho, Y.-H. (2016) Semiconductor photonic nanocavity on a paper substrate. *Adv. Mater.*, **28**, 9765–9769, doi: 10.1002/adma.201603368

22 Watson, J.D. and Crick, F.H.C. (1953) A structure for deoxyribose nucleic acid. *Nature*, **171**, 737–738.

23 Paleček, E. and Bartošík, M. (2012) Electrochemistry of nucleic acids. *Chem. Rev.*, **112**, 3427–3481.

24 Yumusak, C., Singh, T.B., Sariciftci, N.S., and Grote, J.C. (2009) Bio-organic field effect transistors based on crosslinked deoxyribonucleic acid (DNA) gate dielectric. *Appl. Phys. Lett.*, **95**, 263304.

25 Steckl, A.J. (2007) DNA – a new material for photonics? *Nat. Photonics*, **1**, 3–5.

26 Hagen, J.A., Li, W., Steckl, A.J., and Grote, J.G. (2006) Enhanced emission efficiency in organic light-emitting diodes using deoxyribonucleic acid complex as an electron blocking layer. *Appl. Phys. Lett.*, **88** (17), 10–13.

27 Steckl, A.J., Spaeth, H., You, H., Gomez, E., and Grote, G. (2011) DNA as an optical material. *Opt. Photonics News*, **22**, 34.

28 Zhang, Y., Zalar, P., Kim, C., Collins, S., Bazan, G.C., and Nguyen, T.-Q. (2012) DNA interlayers enhance charge injection in organic field-effect transistors. *Adv. Mater.*, **24**, 4255–4260.

29 Irimia-Vladu, M., Troshin, P.A., Reisinger, M., Schwabegger, G., Ullah, M., Schwoediauer, R., Mumyatov, A., Bodea, M., Fergus, J.W., Razumov, V., Sitter, H., Bauer, S., and Sariciftci, N.S. (2010) Environmentally sustainable organic field effect transistors. *Org. Electron.*, **11**, 1974–1990.

30 Irimia-Vladu, M., Troshin, P.A., Reisinger, M., Shmygleva, L., Kanbur, Y., Schwabegger, G., Bodea, M., Schwoediauer, R., Mumyatov, A., Fergus, J.W., Razumov, V., Sitter, H., Sariciftci, N.S., and Bauer, S. (2010) Biocompatible and biodegradable materials for organic field effect transistors. *Adv. Funct. Mat.*, **20** (23), 4069–4076.

31 Irimia-Vladu, M., Sariciftci, N.S., and Bauer, S. (2011) Exotic materials for bio-organic electronics. *J. Mater. Chem.*, **21** (5), 1350–1361.

32 Schwabegger, G., Ullah, M., Irimia-Vladu, M., Baumgartner, M., Kanbur, Y., Ahmed, R., Stadler, P., Bauer, S., Sariciftci, N.S., and Sitter, H. (2011) High mobility, low voltage operating $C_{60}$ based n-type organic field effect transistors. *Synth. Met.*, **161**, 2058–2062.

33 Gomez, E.F., Venkatraman, V., Grote, J.G., and Steckl, A.J. (2014) DNA bases thymine and adenine in bio-organic light emitting diodes. *Sci. Rep.*, **4**, 7105.

34 Gomez, E.F., Venkatraman, V., Grote, J.G., and Steckl, A.J. (2015) Exploring the potential of nucleic acid bases in organic light emitting diodes. *Adv. Mater.*, **27**, 7552–7562.

35 Basu, A. (2015) *Advances in Silk Science and Technology*, Elsevier Science & Technology.

36 Kundu, S. (2014) *Silk Biomaterials for Tissue Engineering and Regenerative Medicine*, Woodhead Publishing Ltd.

37 Hota, M.K., Bera, M.K., Kundu, B., Kundu, S.C., and Maiti, C.K. (2012) A natural silk fibroin protein-based transparent bio-memristor. *Adv. Funct. Mater.*, **22**, 4493–4499.

**38** Magoshi, J. and Magoshi, Y. (1975) Physical properties and structure of silk. II. Dynamic mechanical and dielectric properties of silk fibroin. *J. Polym. Sci., Part B: Polym. Phys.*, **13**, 1347–1351.

**39** Wang, C.-H., Hsieh, C.-Y., and Hwang, J.-C. (2011) Flexible organic thin-film transistors with silk fibroin as the gate dielectric. *Adv. Mater.*, **23**, 1630–1634.

**40** Capelli, R., Amsden, J.J., Generali, G., Toffanin, S., Benfenati, V., Muccini, M., Kaplan, D.L., Omenetto, F.G., and Zamboni, R. (2011) Integration of silk protein in organic and light-emitting transistors. *Org. Electron.*, **12**, 1146–1151.

**41** Chang, T.-H., Liao, C.-P., Tsai, J.-C., Lee, C.-Y., Hwang, J.-C., Tso, I.M., Chueh, Y.-L., Lyu, P.-C., and Gan, J.-Y. (2014) Natural polyelectrolyte: major ampullate spider silk for electrolyte organic field-effect transistors. *Org. Electron.*, **15**, 954–960.

**42** Kim, D.-H., Kim, Y.-S., Amsden, J., Panilaitis, B., Kaplan, D.L., Omenetto, F.G., Zakin, M.R., and Rogers, J.A. (2009) Silicon electronics on silk as a path to bioresorbable, implantable devices. *Appl. Phys. Lett.*, **95**, 133701.1–133701.3.

**43** Hwang, S.-W., Tao, H., Kim, D.-H., Cheng, H., Song, J.-K., Rill, E., Brenckle, M.A., Panilaitis, B., Won, S.M., Kim, Y.-S., Song, Y.M., Yu, K.J., Ameen, A., Li, R., Su, Y., Yang, M., Kaplan, D.L., Zakin, M.R., Slepian, M.J., Huang, Y., Omenetto, F.G., and Rogers, J.A. (2012) A physically transient form of silicon electronics. *Science*, **337**, 1640–1644.

**44** Müller, C., Hamedi, M., Karlsson, R., Jansson, R., Marcilla, R., Hedhammar, M., and Inganäs, O. (2011) Woven electrochemical transistors on silk fibers. *Adv. Mater.*, **23**, 898–901.

**45** Marggraf, A.S. (1747) *Experiences Chimiques Faites Dans le Dessein de Tirer un Veritable Sucre de Diverses Plantes, qui Croissent Dans nos Contrées*, vol. **2**, Histoire de l'académie Royale des Sciences et Belles-lettres de Berlin, pp. 79–90; Chymische Schriften 1767.

**46** Acar, H., Çınar, S., Thunga, M., Kessler, M.R., Hashemi, N., and Montazami, R. (2014) Study of physically transient insulating materials as a potential platform for transient electronics and bioelectronics. *Adv. Funct. Mater.*, **24**, 4135–4143.

**47** Surjushe, A. and Vasani, R. (2008) Aloe Vera: a short review. *Indian J. Dermatol.*, **53** (4), 163–166.

**48** Khor, L.Q. and Cheong, K.Y. (2013) Aloe Vera gel as natural organic dielectric in electronic application. *J. Mater. Sci. – Mater. Electron.*, **24** (7), 2646–2652.

**49** Qian Khor, L. and Yew Cheong, K. (2013) N-type organic field-effect transistor based on fullerene with natural aloe vera/SiO2 nanoparticles as gate dielectric. *ECS J. Solid State Sci. Technol.*, **2** (11), P440–P444.

**50** Kennedy, J.F., Phillips, G.O., and Williams, P.A. (2015) *Gum Arabic: RSC (Special Publication)*, vol. **1**, Royal Society of Chemistry.

**51** Montenegro, M.A., Boiero, M.L., Valle, L., and Borsarelli, C.D. (2012) Gum arabic : more than an edible emulsifier. *Prod. Appl. Biopolym.*, **17** (3), 220.

**52** Paraschos, S., Mitakou, S., and Skaltsounis, A.L. (2012) Chios gum mastic: a review of its biological activities. *Curr. Med. Chem.*, **19**, 2292–2302.

**53** Lakkis, J.M. (2016) *Encapsulation and Controlled Release Technologies in Food Systems*, John Wiley & Sons, Inc., pp. 289–308.

**54** Stadlober, B., Karner, E., Petritz, A., Fian, A., and Irimia-Vladu, M. (2015) Nature as microelectronic fab: bioelectronics: materials, transistors and circuits. *IEEE European Solid-State Device Research Conference 2015*, pp. 10–17

55 Glowacki, E.D., Irimia-Vladu, M., Kaltenbrunner, M., Gsiorowski, J., White, M.S., Monkowius, U., Romanazzi, G., Suranna, G.P., Mastrorilli, P., Sekitani, T., Bauer, S., Someya, T., Torsi, L., and Sariciftci, N.S. (2013) Hydrogen-bonded semiconducting pigments for air-stable field-effect transistors. *Adv. Mater.*, **25** (11), 1563–1569.

56 Steckl, A.J. (2013) Circuits on cellulose. *IEEE Spectr.*, **50** (2), 48–61.

57 Petritz, A., Wolfberger, A., Fian, A., Irimia-Vladu, M., Haase, A., Gold, H., Rothländer, T., Griesser, T., and Stadlober, B. (2013) Cellulose as biodegradable high-k dielectric layer in organic complementary inverters. *Appl. Phys. Lett.*, **103**, 153303.

58 Petritz, A., Wolfberger, A., Fian, A., Griesser, T., Irimia-Vladu, M., and Stadlober, B. (2015) Cellulose-derivative-based gate dielectric for high-performance organic complementary inverters. *Adv. Mater.*, **27**, 7645–7656.

59 Petritz, A., Fian, A., Glowacki, E.D., Sariciftci, N.S., Stadlober, B., and Irimia-Vladu, M. (2015) Ambipolar inverters with natural origin organic materials as gate dielectric and semiconducting layer. *Phys. Status Solidi RRL*, **9**, 358–361.

60 Thiemann, S., Sachnov, S.J., Pettersson, F., Bollström, R., Österbacka, R., Wasserscheid, P., and Zaumseil, J. (2013) Cellulose-based ionogels for paper electronics. *Adv. Funct. Mater.*, **24** (5), 625–634.

61 Gomez, E.F. and Steckl, A.J. (2015) Improved performance of OLEDs on cellulose/epoxy substrate using adenine as a hole injection layer. *ACS Photonics*, **2** (3), 439–445.

62 Klemm, D., Kramer, F., Moritz, S., Lindström, T., Ankerfors, M., Gray, D., and Dorris, A. (2011) Nanocelluloses: a new family of nature-based materials. *Angew. Chem. Int. Ed.*, **50** (24), 5438–5466.

63 Mautner, A., Lee, K.Y., Tammelin, T., Mathew, A.P., Nedoma, A.J., Li, K., and Bismarck, A. (2015) Cellulose nanopapers as tight aqueous ultra-filtration membranes. *React. Funct. Polym.*, **86**, 209–214.

64 Lee, K.Y., Buldum, G., Mantalaris, A., and Bismarck, A. (2014) More than meets the eye in bacterial cellulose: biosynthesis, bioprocessing, and applications in advanced fiber composites. *Macromol. Biosci.*, **14** (1), 10–32.

65 Mantell, C.L. (1950) The natural hard resins—their botany, sources and utilization. *Econ. Bot.*, **4**, 203–242.

66 Langenheim, J.H. (2003) *Plant Resins: Chemistry, Evolution, Ecology and Ethnobotany*, Timber Press Inc..

67 Hicks, E. (1962) *Shellac: its origin and applications*, MacDonald & Co.

68 Bose, P.K., Sankaranarayanan, Y., and Sen Gupta, S.C. (1963) *Chemistry of Lac*, Indian Research Institute.

69 Hagenmaier, R.D. and Shaw, P.E. (1991) Permeability of shellac coatings to gases and water vapor. *J. Agric. Food. Chem.*, **39**, 825–829.

70 Goswami, D.N. (1979) Dielectric behavior of the constituents of the natural resin shellac. *J. Appl. Polym. Sci.*, **24**, 1977–1984.

71 Irimia-Vladu, M., Glowacki, E.D., Schwabegger, G., Leonat, L., Akpinar, H.Z., Sitter, H., Bauer, S., and Sariciftci, N.S. (2013) Natural resin shellac as a substrate and a dielectric layer for organic field-effect transistors. *Green Chem.*, **15**, 1473–1476.

72 Irimia-Vladu, M., Glowacki, E.D., Troshin, P.A., Schwabegger, G., Leonat, L., Susarova, D.K., Krystal, O., Ullah, M., Kanbur, Y., Bodea, M.A., Razumov, V.F.,

Sitter, H., Bauer, S., and Sariciftci, N.S. (2012) Indigo-a natural pigment for high performance ambipolar organic field effect transistors and circuits. *Adv. Mater.*, **24**, 375–380.

**73** Schrieber, R. and Gareis, H. (2007) *Gelatine Handbook: Theory and Industrial Practice*, Wiley-VCH Verlag GmbH.

**74** Mao, L.K., Hwang, J.C., Chang, T.H., Hsieh, C.Y., Tsai, L.S., Chueh, Y.L., Hsu, S.S.H., Lyu, P.C., and Liu, T.J. (2013) Pentacene organic thin-film transistors with solution-based gelatin dielectric. *Org. Electron. Appl.*, **14** (4), 1170–1176.

**75** Mao, L.K., Hwang, J.C., and Tsai, J.C. (2015) Operation voltage reduction and gain enhancement in organic cmos inverters with the ttc/gelatin bilayer dielectric. *Org. Electron.*, **16**, 221–226.

**76** Paradossi, G., Cavalieri, F., Chiessi, E., Spagnoli, C., and Cowman, M.Y. (2003) Poly(vinyl alcohol) as versatile biomaterial for potential biomedical applications. *J. Mater. Sci. – Mater. Med.*, **14**, 687–691.

**77** Wang, X., Xu, W., Chatterjee, P., Lv, C., Popovich, J., Song, Z., Dai, L., Kalani, M.Y.S., Haydel, S.E., and Jiang, H. (2016) Food-materials-based edible supercapacitors. *Adv. Mater. Technol.*, **1**, 1–7.

**78** Chang, J.W., Wang, C.G., Huang, C.Y., Da Tsai, T., Guo, T.F., and Wen, T.C. (2011) Chicken albumen dielectrics in organic field-effect transistors. *Adv. Mater.*, **23** (35), 4077–4081.

**79** Wu, G., Feng, P., Wan, X., Zhu, L., Shi, Y., and Wan, Q. (2016) Artificial synaptic devices based on natural chicken albumen coupled electric-double-layer transistors. *Sci. Rep.*, **6**, 23578.

**80** Dezieck, A., Acton, O., Leong, K., Oren, E.E., Ma, H., Tamerler, C., Sarikaya, M., and Jen, A.K.Y. (2010) Threshold voltage control in organic thin film transistors with dielectric layer modified by a genetically engineered polypeptide. *Appl. Phys. Lett.*, **97** (1), 1–4.

**81** Tang, C.W. and Albrecht, A.C. (1975) Photovoltaic effects of metal–chlorophyll-a–metal sandwich cells. *J. Chem. Phys.*, **62** (6), 2139–2149.

**82** Moses, D., Heeger, A.J., Cornil, J., and Brddas, J.L. (1992) Doped beta-carotene films: spinless charge storage stabilized by structural relaxation. *Chem. Phys. Lett.*, **196** (1), 84–90.

**83** Glowacki, E.D., Leonat, L., Voss, G., Bodea, M., Bozkurt, Z., Irimia-Vladu, M., Bauer, S., and Sariciftci, N.S. (2011) Natural and nature-inspired semiconductors for organic electronics. *Proceedings of SPIE 2011, vol. 8118, 81180M–81180M–10*.

**84** Wang, X., Wang, L., Wang, Z., Wang, Y., Tamai, N., Hong, Z., and Kido, J. (2013) Natural photosynthetic carotenoids for solution-processed organic bulk-heterojunction solar cells. *J. Phys. Chem. C*, **117**, 804–811.

**85** Bechtold, T. and Mussak, R. (2009) *Handbook of Natural Colorants*, John Wiley & Sons, Ltd., Chichester.

**86** Ferreira, E.S.B., Hulme, A.N., McNab, H., and Quye, A. (2004) The natural constituents of historical textile dyes. *Chem. Soc. Rev.*, **33** (6), 329–336.

**87** Glowacki, E.D., Irimia-Vladu, M., Bauer, S., and Sariciftci, N.S. (2013) Hydrogen-bonds in molecular solids – from biological systems to organic electronics. *J. Mater. Chem. B*, **1** (31), 3742–3753.

88 Aakeroy, C.B. and Seddon, K.R. (1993) The hydrogen bond and crystal engineering. *Chem. Soc. Rev.*, **22**, 397–407.

89 Desiraju, G.R. (2011) Reflections on the hydrogen bond in crystal engineering. *Cryst. Growth Des.*, **11** (4), 896–898.

90 Glowacki, E.D., Voss, G., and Sariciftci, N.S. (2013) 25th anniversary article: progress in chemistry and applications of functional indigos for organic electronics. *Adv. Mater.*, **25** (47), 6783–6800.

91 Seefelder, M. (1994) *Indigo in Culture, Science, and Technology*, Ecomed, Landsberg.

92 Zollinger, H. (2003) *Color Chemistry. Syntheses, Properties and Applications of Organic Dyes and Pigments*, Wiley-VCH Verlag GmbH, Weinheim.

93 Steingruber, E.Indigo Indigo Color. (2007) *Ullmann's Encyclopedia of Industrial Chemistry*, Wiley-VCH Verlag GmbH, Weinheim, pp. 1–9.

94 Glowacki, E.D., Leonat, L.N., Voss, G., Badea, M., Bozkurt, Z., Irimia-Vladu, M., Bauer, S., and Sariciftci, N.S. (2011) Ambipolar organic field effect transistors and inverters with the natural material tyrian purple. *AIP Adv.*, **1**, 042132–042137.

95 Kanbur, Y., Irimia-Vladu, M., Glowacki, E.D., Baumgartner, M., Schwabegger, G., Leonat, L.N., Ullah, M., Sitter, H., Schwödiauer, R., Kücükyavuz, Z., Bauer, S., and Sariciftci, N.S. (2012) Vacuum processed polyethylene as a dielectric for low voltage operating organic field effect transistors. *Org. Electron.*, **13**, 919–924.

96 Đerek, V., Glowacki, E.D., Sytnyk, M., Heiss, W., Marciuš, M., Ristić, M., Ivanda, M., and Sariciftci, N.S. (2015) Enhanced near-infrared response of nano- and microstructured silicon/organic hybrid photodetectors. *Appl. Phys. Lett.*, **107**, 83302.

97 Scherwitzl, B., Resel, R., and Winkler, A. (2014) Film growth, adsorption and desorption kinetics of indigo on $SiO_2$. *J. Chem. Phys.*, **140** (18), 184705.

98 Truger, M., Roscioni, O.M., Röthel, C., Kriegner, D., Simbrunner, C., Ahmed, R., Glowacki, E.D., Simbrunner, J., Salzmann, I., Coclite, A.M., Jones, A.O.F., and Resel, R. (2016) Surface-induced phase of tyrian purple (6,6′-Dibromoindigo): thin film formation and stability. *Cryst. Growth Des.*, **16**, 3647–3655.

99 Anokhin, D.V., Leshanskaya, L.I., Piryazev, A., Susarova, D.K., Dremova, N.N., Shcheglov, E.V., Ivanov, D.A., Razumov, V.F., and Troshin, P.A. (2014) Towards understanding the behavior of indigo thin films in organic field-effect transistors: a template effect of the aliphatic hydrocarbon dielectric on the crystal structure and electrical performance of the semiconductor. *Chem. Commun.*, **50** (57), 7639–7641.

100 Klimovich, I.V., Leshanskaya, L.I., Troyanov, S.I., Anokhin, D.V., Novikov, D.V., Piryazev, A.A., Ivanov, D.A., Dremova, N.N., and Troshin, P.A. (2014) Design of indigo derivatives as environment-friendly organic semiconductors for sustainable organic electronics. *J. Mater. Chem. C*, **2** (36), 7621–7631.

101 Pitayatanakul, O., Higashino, T., Kadoya, T., Tanaka, M., Kojima, H., Ashizawa, M., Kawamoto, T., Matsumoto, H., Ishikawa, K., and Mori, T. (2014) High performance ambipolar organic field-effect transistors based on indigo derivatives. *J. Mater. Chem. C*, **2** (43), 9311–9317.

**102** Herbst, W. and Hunger, K. (2004) *Industrial Organic Pigments*, Wiley-VCH Verlag GmbH, Weinheim.

**103** Klebe, G., Graser, F., Hädicke, E., and Berndt, J. (1989) Crystallochromy as a solid-state effect: correlation of molecular conformation, crystal packing and colour in perylene-3,4:9,10-bis(dicarboximide) pigments. *Acta Crystallogr., Sect. B: Struct. Sci*, **45** (1), 69–77.

**104** Faulkner, E.B. and Schwartz, R.J. (eds) (2009) *High Performance Pigments*, Wiley-VCH Verlag GmbH, Weinheim.

**105** Hunger, K. (2005) Toxicology and toxicological testing of colorants. *Rev. Prog. Color. Relat. Top.*, **35**, 76–89.

**106** Labana, S.S. and Labana, L.L. (1967) Quinacridones. *Chem. Rev.*, **67** (1), 1–18.

**107** Glowacki, E.D., Leonat, L., Irimia-Vladu, M., Schwödiauer, R., Ullah, M., Sitter, H., Bauer, S., and Sariciftci, N.S. (2012) Intermolecular hydrogen-bonded organic semiconductors—quinacridone versus pentacene. *Appl. Phys. Lett.*, **101** (2), 23305.

**108** Haucke, G. and Graness, G. (1995) Thermal isomerization of indigo. *Angew. Chem.*, **34** (1), 67–68.

**109** Glowacki, E.D., Romanazzi, G., Yumusak, C., Coskun, H., Monkowius, U., Voss, G., Burian, M., Lechner, R.T., Demitri, N., Redhammer, G.J., Sünger, N., Suranna, G.P., and Sariciftci, N.S. (2015) Epindolidiones-versantile and stable hydrogen-bonded pigments for organic field-effect transistors and light-emitting diodes. *Adv. Funct. Mater.*, **25**, 776–787.

**110** Rossi, L., Bongiovanni, G., Kalinowski, J., Lanzani, G., Mura, A., Nisoli, M., and Tubino, R. (1996) Ultrafast optical probes of electronic excited states in linear trans-quinacridone. *Chem. Phys. Lett.*, **257**, 545–551.

**111** Glowacki, E.D., Tangorra, R.R., Coskun, H., Farka, D., Operamolla, A., Kanbur, Y., Milano, F., Giotta, L., Farinola, G.M., and Sariciftci, N.S. (2015) Bioconjugation of hydrogen-bonded organic semiconductors with functional proteins. *J. Mater. Chem. C*, **3**, 6554–6564.

**112** Jakešová, M., Apaydin, D.H., Sytnyk, M., Oppelt, K., Heiss, W., Sariciftci, N.S., and Glowacki, E.D. (2016) Hydrogen-bonded organic semiconductors as stable photoelectrocatalysts for efficient hydrogen peroxide photosynthesis. *Adv. Funct. Mater.*, **26**, 5248–5254.

**113** Wang, C., Zhang, Z., and Wang, Y. (2016) Quinacridone-based π-conjugated electronic materials. *J. Mater. Chem. C*, **4**, 9918–9936.

**114** Kotwica, K., Bujak, P., Wamil, D., Materna, M., Skorka, L., Gunka, P.A., Nowakowski, R., Golec, B., Luszczynska, B., Zagorska, M., and Pron, A. (2014) Indanthrone dye revisited after sixty years. *Chem. Commun.*, **50** (78), 11543–11546.

**115** Kotwica, K., Bujak, P., Data, P., Krzywiec, W., Wamil, D., Gunka, P.A., Skorka, L., Jaroch, T., Nowakowski, R., Pron, A., and Monkman, A. (2016) Soluble flavanthrone derivatives: synthesis, characterization, and application to organic light-emitting diodes. *Chem. A Eur. J.*, **22**, 7978–7986.

**116** Zambounis, J.S., Hao, Z., and Iqbal, A. (1997) Latent pigments activated by heat. *Nature*, **388**, 131–132.

**117** Hao, Z. and Iqbal, A. (1997) Some aspects of organic pigments. *Chem. Soc. Rev.*, **26** (3), 203.

**118** Glowacki, E.D., Voss, G., Demirak, K., Havlicek, M., Sünger, N., Okur, A.C., Monkowius, U., Gąsiorowski, J., Leonat, L., and Sariciftci, N.S. (2013) A facile protection–deprotection route for obtaining indigo pigments as thin films and their applications in organic bulk heterojunctions. *Chem. Commun.*, **49**, 6063–6065.

**119** Glowacki, E.D., Apaydin, D.H., Bozkurt, Z., Monkowius, U., Demirak, K., Tordin, E., Himmelsbach, M., Schwarzinger, C., Burian, M., Lechner, R.T., Demitri, N., Voss, G., and Sariciftci, N.S. (2014) Air-stable organic semiconductors based on 6,6′-dithienylindigo and polymers thereof. *J. Mater. Chem. C*, **2** (38), 8089–8097.

**120** Sytnyk, M., Daniel, E., Yakunin, S., Voss, G., Schöfberger, W., Kriegner, D., Stangl, J., Trotta, R., Gollner, C., Tollabimazraehno, S., Romanazzi, G., Bozkurt, Z., Havlicek, M., Sariciftci, N.S., and Heiss, W. (2014) Hydrogen-bonded organic semiconductor micro- and nanocrystals: from colloidal syntheses to (opto-)electronic devices. *J. Am. Chem. Soc.*, **136**, 16522–16532.